

SCP

CERN - SPSC - 98-24

84 9306

CERN LIBRARIES, GENEVA



SC00001001

CERN/SPSC 98-24

SPSC/M611

22.09.1998

MICROMEAS STATUS REPORT

Presented by Y. Giomataris

A. Baldisseri, J. Ball, G. Barouch, Ph. Briet, M. Combet, J. Derré,
R. Durand, J.C. Faivre, A. Giganon, Y. Giomataris, J. Gosset, D. Jourde,
C. Kochowski, F. Kunne, J.M. Le Goff, F. Lehar, Y. Lemoigne,
S. Loucatos, J.C. Lugol, A. Magnon, B. Mayer, S. Platchkov, G. Puill,
Ph. Rebourgeard, J.-P. Robert, Y. Terrien, D. Thers, H. Zaccane

*CEA/DSM/DAPNIA-C.E.-Saclay
91191 Gif/Yvette, France*

G. Charpak

*Ecole Supérieure de Physique et Chimie Industrielle de la Ville de Paris, ESPCI,
Paris
and CERN/AT, Geneva*

A. Bay, R. Frei, J.P. Perroud

Lausanne University

F. Didierjean

EURISYS Mesures, Strasbourg

J.-C. Fontaine, D. Huss, F. Jeanneau

Mulhouse University

CERN LIBRARIES, GENEVA



SC00000952

ABSTRACT

We describe results obtained using a novel structure of a gaseous detector, called MICROMEGAS [1] which is under development at Saclay. It consists of a two stage parallel plate avalanche chamber having a small amplification gap of $100\ \mu\text{m}$, combined with a conversion-drift space of $3\ \text{mm}$. The anode plane is made of microstrips, $317.5\ \mu\text{m}$ pitch, printed on a thin substrate. Fast signals are obtained during the collection ($1\ \text{ns}$) of the electron avalanche on the anode microstrip plane, while positive ions are fully collected within $100\ \text{ns}$. The fast evacuation of the ion space charge and the high granularity of the detector opens the way to achieve very high counting rates. The rate capability is measured with $10\ \text{MeV}$ protons from a TANDEM accelerator, a $8\ \text{keV}$ X-ray generator and high energy minimum ionising particles. No saturation of the gain is observed up to $10^9\ \text{particles}/\text{mm}^2/\text{s}$. With Argon and DME filling the gain is stable up to $50\ \text{mC}$ total charge on a $3\ \text{mm}^2$ area. It corresponds to about 10 years for a detector located at $40\ \text{cm}$ from the beam pipe of the LHC collider, running at its full luminosity.

The device is constructed using known technology, it is easy to operate and cost effective. Several $15 \times 15\ \text{cm}^2$ chambers have been tested in a $100\ \text{GeV}/c$ muon beam at high rates up to $10^8/\text{s}$ over a surface of $2\ \text{cm}^2$ under stable and safe conditions.

A systematic research on gases shows the favorable characteristics of Argon + Cyclohexane allowing gains above 10^5 under stable conditions, with a plateau of $50\ \text{V}$ at $340\ \text{V}$. With the addition of CF_4 a time resolution of $5\ \text{ns}$ (RMS) is reached.

Spatial resolution of $60\ \mu\text{m}$ has been measured.

Amplification gaps of $50\ \mu\text{m}$ show an improvement in all the characteristics of Micromegas. With a conversion gap of $1\ \text{mm}$ the efficiency reaches 96% .

Preliminary results inside a magnet show stable operation of the detector up to $1.3\ \text{Tesla}$.

1 Introduction

A great effort has been invested the last 10 years to develop gaseous detectors capable to operate in high rate environments, with particle flux beyond 10^4 particles/mm²/s, which is the limit of operation of conventional MWPCs[2]. The motivation is great for both future high energy physics projects or contemporary medical radiography.

To overcome these limitations, a new technique, the microstrip gas chamber (MSGC), has been intensively developed [3–5]. Wires are replaced by strips printed on an insulating support; a high electric field region, sufficient for electron multiplication, is created between the thin cathode and anode conductive strips. The small inter-strip pitch allows a good spatial resolution, inferior to $100\ \mu\text{m}$ and the fast collection of the charges offers the possibility to cope with higher counting rates. One limitation of the MSGC detector is the fact that the avalanche multiplication does not exceed 10^4 , because of breakdown on the insulator surface. Positive ions created during the avalanche process and accumulated on the insulator, locally modify the electric field and cause a drop of the gain in the irradiated area of the detector[6]. A lot of effort has been invested, during the last few years, to resolve the charging-up problem by a careful choice of the resistivity of the substrate or a special treatment of its surface.

Another possible way out is the use of a special asymmetric configuration of the multiwire structure[7,8] with alternating anodes and field-shaping wires, mounted close to the cathode plane with engraved pick-up strips orthogonal to the wire direction. The performance of this structure equals that of the MSGC in terms of rate capability and spatial resolution. In addition it can achieve higher electron multiplication factors and it operates in a stable fashion for long irradiation periods. The drawback here is the use of delicate wires and the wire stretching force, which is proportional to the total number of wires acting in the wire frame; this therefore has to be of substantial thickness.

Micromegas [1] is a new gaseous detector based on simple geometry with planar electrodes. It consists of a conversion gap in which radiations liberate ionization electrons and of a thin amplification gap. The two regions are separated by a thin ($3\ \mu\text{m}$) grid. The free electrons drift into the amplification gap where printed electrodes of any shape collect the electrons from the avalanche.

We had come to the conclusion, in our first tests [9], that it is possible to build chambers of sizes adapted to the future high luminosity detectors, with high count rates capability and good time and space resolution.

2 Detector description

The device operates as a two-stage parallel plate avalanche chamber and it is called MICROME GAS (MICRO-MESH-GASEOUS STRUCTURE). It is a miniaturized version of a very asymmetric two-stage parallel plate detector. A micromesh separates the conversion space, of about 3 mm, from a small amplification gap that can be as small as $50\ \mu\text{m}$. Figure 1 shows a schematic representation of a typical detector. It consists of the following components:

- (i) The anode electrode. Copper strips of $250\ \mu\text{m}$, with $317\ \mu\text{m}$ pitch, are printed on a $1.6\ \text{mm}$ substrate. The thickness of the copper strip is $5\ \mu\text{m}$.
- (ii) The micromesh. It is a metallic grid, $3\ \mu\text{m}$ thick, with $37\ \mu\text{m}$ openings every $50\ \mu\text{m}$. It is made of nickel, using the electroforming technique. The use of the photographic process and especially high-resolution emulsions, ensures a high precision, better than $1\ \mu\text{m}$. The optical transparency was measured to be 59%. The flatness of the micromesh and therefore the accuracy of the amplification gap is assured by cylindrical insulating pillars, $2\ \text{mm}$ spaced, $100\ \mu\text{m}$ thick, $200\ \mu\text{m}$ in diameter, printed on top of the anode strips using standard lithography.
- (iii) The drift electrode. It consists of a 2 micron aluminized mylar or a thin capton foil at a distance of about $3\ \text{mm}$ from the micromesh. On this electrode a negative potential (HV1) slightly higher than the micromesh voltage (HV2) is applied, to define a uniform conversion-drift electric field.

Ionization electrons, created by the energy deposition of an incident charged particle in the conversion gap, drift and can be transferred through the cathode micromesh; they are amplified in the small gap, between anode and cathode, under the action of the electric field, which is high in this region. The electron cloud is finally collected by the anode microstrips, while the positive ions are drifting in the opposite direction and are collected on the micromesh. This configuration allows us to obtain, by applying reasonable voltages in the three electrodes, a very high electric field in the amplification region ($50\text{-}100\ \text{kV/cm}$) and a quite low electric field in the drift region. Therefore, the ratio between the electric field in the amplification gap and that in the conversion gap can be tuned to large values, as is required for an optimal operation of the device. Such a high ratio is also required in order to catch the ions in the small amplification gap: under the action of the high electric field, the ion cloud is quickly collected on the micromesh and only a small part of it, inversely proportional to the electric field ratio, escapes to the conversion region.

The electric field must be uniform in both conversion and amplification spaces. This is easily obtained by using the micromesh as the middle electrode. The electric-field shape is, however, disturbed close to the holes of the micromesh. The knowledge of the shape of the field lines close to the micromesh is a fundamental issue for the operation of our detector, and especially for the efficiency of the passage of electrons through the micromesh, as well as, for the fast evacuation of the positive-ion build-up. The electric field exhibits a funnel like shape very close to the openings of the microgrid: field lines are compressed towards the middle of the openings into a small diameter of the order of a few microns, depending on the electric field ratio between the two gaps. All the electrons liberated in the conversion gap by the ionizing radiation are focused into the multiplication gap. Figure 2 displays details field lines near the grid used in the present tests ($50\ \mu\text{m}$ opening pitch).

An interesting property of Micromegas is that small variations of the amplification gap, due to mechanical defects, are compensated by an inverse variation of the amplification factor. As shown in Figure 3, for a given voltage applied in a thin parallel plate chamber, the gain as a function of the gap width presents a maximum around 50 to 100 microns. Micromegas which operates in this region is therefore not sensitive to defects of flatness and is optimal for parallel-plate avalanche mode, resulting in a rather large dynamic range for the amplification before breakdown.

3 Energy resolution

The energy resolution of the detector was measured using the ^{55}Fe radioactive source. The obtained pulse-height distribution is shown in Figure 4. One can easily separate the 5.9 keV peak and the Ar escape peak at 2.7 keV. The energy resolution obtained, 14% (FWHM), is more than satisfactory. It shows that the detector can achieve a good homogeneity of the gain, in spite of possible fluctuations due to mechanical misalignments inside the micro-amplification gap.

4 Gas gain

In order to improve spatial resolution we have to use gas mixtures of smaller transverse diffusion and smaller strips. A laboratory study has been undertaken to optimize the primary ionization, drift and diffusion of the electrons and the gas amplification process. The last three parameters are closely linked to the nature of the gas mixture. In such a detector, designed for high rate particle environments, it is important to find a gas mixture which allows a high gain, around 10^5 : although the gain range of operation will be between 10^3 and 10^4 , a higher maximum gain gives the necessary margin, to prevent sparks in the detector. Moreover, the gas mixture must have a drift velocity as high as possible to improve the time resolution.

Several gas mixtures have been tested and detailed results will be published in a coming paper.

We have worked with Argon + Cyclohexane mixture with a possible adjunction of CF_4 . Cyclohexane, at room temperature is a liquid.

Bubbling Argon through Cyclohexane at controlled temperature we can vary the proportion of vapors which is 8% at 15°C . At a pressure of 1 bar we can see (Figure 5) the dependence of the gain which can be reached as a function of Cyclohexane concentration in Argon, with a $50\ \mu\text{m}$ gap. The optimum is around 3% and permits a maximum gain of 3.5×10^5 .

The admixture of various proportions of CF_4 has a strong influence on both electron drift velocity and electron diffusion in the conversion gap: electron velocity increases and the diffusion coefficient decreases. With 20% of CF_4 admixture the maximum gain is still high, 1.5×10^5 . The most promising mixture is pure CF_4 and a small proportion of Cyclohexane. The maximum gain achieved with 7% Cyclohexane is high, 7×10^4 , when the detector is irradiated with 5.9 keV X-rays and is still significant, 10^4 as shown in Figure 6, at high flux $5 \times 10^5/\text{mm}^2/\text{s}$ in a 8 KeV X-ray environment.

This mixture yields the highest drift velocity, $2 \times 10^7\text{cm/s}$, allowing excellent time properties and the diffusion is expected to be as low as 70 micron per 1 cm path [12]. It also increases the number of primary ionization collisions by two and the total primary electrons by three compared to the standard Argon and Isobutane gas mixture. Using CF_4 as carrier gas, one can further reduce the conversion gap below 1 mm and still keep full efficiency of the detector. Such a small gap will limit the degradation of the spatial resolution due to inclined tracks or the presence of strong magnetic field and will improve its time resolution.

5 Signal development and electronics

The signal induced on the anode strips is a sum of the electron and ion signal.

The charge induced during the avalanche can be entirely measured using a low-noise charge preamplifier. The charge signal is mainly due to the positive ion drift to the micromesh electrode, which takes place typically within 100 ns, depending on the width of the amplification gap. Figure 7 shows signals coming out from a charge-sensitive preamplifier for an Argon + 10% Isobutane gas mixture. The rise reflects the total ion drift and it is 100 ns for the 100 micron and only about 30 ns for the 50 micron amplification gap. So, for the latter case, shaping of the signal around 30 ns allows to catch the full induced charge and therefore permits a comfortable operation of the detector at moderate gains of the order of 3000. Electronics chips, giving a good signal-to-noise ratio in Micromegas, are those currently under development for silicon microstrip detectors.

As far as the current signal is concerned the highest amplitude is due to the electron drift because of its higher drift velocity (about 100 times faster than the ion drift). As shown in Figure 8 the calculated current exhibits a very fast rise (within 1 ns) and a tail due to the ion drift. The very fast electron signal is quite difficult to catch, but is within reach with present electronics. The deal is illustrated in Figure 9 showing signals taken using a commercially available Lecroy-MQS104A chip (10 ns rise), during a high rate beam test in the SPS at CERN. The figure shows two signals, simultaneously taken from two detectors with respectively 100 and 50 micron amplification gap. The first signal has a fast rise due to the electron current and a longer tail due to the ion current. In the second signal the ion tail is reduced, but the fast component is still weaker than expected. Using however, a new preamplifier with faster rise (1 ns) the result is spectacular (Figure 10) : the fast electron signal is much steeper (rise about 1 ns), still dominated by the electronics speed. But, the fast signal is now 10 times higher than the ion tail.

In conclusion, for most of the present applications (LHC experiments or other high radiation environments) existing charge preamplifiers with a typical integration time of about 30 ns will permit a comfortable operation of the detector, while fast (10 ns) current preamplifiers (such developed for MWPC counters) are not adequate for our detector.

In the following sections we present experimental results obtained in two particle beams at CERN. In the first test (PS beam), charge preamplifiers have been used, providing a large detection plateau, while in the second run (SPS intense beam) where we used MQS104A chips the result was good but the efficiency plateau rather marginal.

6 Beam tests at moderate particle flux

6.1 Set-up

Our first tests of Micromegas were done with a gas filling of Argon-Isobutane [9]. We pursued with a more standard Argon-DME mixture. The amplification gap was 100

μm .

The Micromegas detectors were on a platform between two drift chambers 3 m apart, giving two co-ordinate accuracy of $150 \mu\text{m}$. An event was triggered by a coincidence between scintillation counters upstream and downstream of the platform, defining a beam area of 2 cm^2 in a CERN PS test beam (T9) of 10 GeV/c negative pions, diverging by 2 mrd horizontally and 1 mrd vertically.

Tests were made first with a doublet of Micromegas, with adjacent rear planes against each other, thus putting the detecting planes (middle of drift gap) at a distance of 9 mm. With this set-up we tested the characteristics of Micromegas with respect to the amplification gain and to different mixtures of Argon-DME.

Then a Micromegas which can turn around an horizontal axis (along the strip direction), was placed in the middle of the platform, sandwiched by two Micromegas doublets 25 cm apart. Rotating the Micromegas in the middle of this second set-up and using the two doublets as a telescope, we measured the dependence of the spatial resolution with respect to the track angle.

All the detectors Micromegas had an active surface of $15 \times 15 \text{ cm}^2$, but only the central part of the strips was electronically equipped (96 strips per plane).

Three chips of 16 charge preamplifiers, of the multiplexed electronics Gassiplex, were connected in serial on each side of the detector. So 48 signals of one over two strip were multiplexed in time on one output to be read out in the ADC. On each strip, we measured an Equivalent Noise Charge (ENC) of 1500 electrons.

6.2 Analysis

As a preliminary feature, we point out that the amplification gain deduced from the collected charge on strips is 7 times lower than the gain measured in laboratory with the signal induced on the mesh by a Fe^{55} source (Figure 11). The biggest part of the strip signal loss was explained a posteriori in laboratory, by a bad timing in the peaking time of Gassiplex which was set at $1 \mu\text{s}$ instead of 400 ns, and by a loss in the 30 m cables. Nevertheless the two exponential slopes of the gain versus the mesh potential are in good agreement, which means that Micromegas was working as expected.

A second remark concerns the choice of the threshold in the search of clusters. This choice is a compromise between a low threshold to insure a good efficiency or a higher one to reduce the number of noisy strips. On Figure 12 it is clear that a reasonable cut is between 3 and 6 (in pedestal standard deviation units). For most of the following we have chosen a threshold at 3. Note that the noise at high cut doesn't drop to zero. This is due to remaining double tracks encoded by the Gassiplex electronics which has a long integration time of the order of 600 ns.

Another interesting feature is the good uniformity of the Micromegas response (Figure 13), except in the pillar zones. The spacers ($200 \mu\text{m}$ diameter), which maintain the $100 \mu\text{m}$ gap between the micromesh and the strips, are disposed every 2 mm, aligned on every 6th strip. On enclosed Figure 13 we see the effect of the spacers. They induce a loss on signal of 7% on the strips (modulo 6) where they lay, as expected from the geometrical acceptance. The resulting efficiency loss is negligible, less than 1%.

6.2.1 Efficiency

In the first data, the drift voltage is fixed at 850 Volts. With the gas mixture of 90% Argon and 10% DME, we observe an efficiency plateau of 25 Volts (Figure 14) at a level of 99%. Beyond a gain of 35000 reached at 395 Volts, we observed an increase in the frequency of sparks. Although they are not destructive, neither for the chamber nor the electronics, we stop at this level. As mentioned previously, we have lost a factor 7 in the signal. So in fact, the length of the plateau should be significantly larger.

A typical distribution of the collected charge is shown in the enclosed Figure 14. The ratio of the charge of the cluster (S) to the noise (N) of a strip is 40 at the peak for 395 Volts. This shape looks like a Landau distribution as expected by the fluctuation in the number of electrons created in the conversion gap.

6.2.2 Cluster size

The size of a cluster on a track is defined as the number of adjacent strips with collected charge above 3 ENC, the cut we used in the analysis. The cluster size grows smoothly with the mesh potential (Figure 15) from 2 at the beginning of the efficiency plateau to 2.7 at the end. It means the strip pitch is well adapted to these operating conditions.

6.2.3 Spatial resolution

The spatial resolution is determined with the doublet of detectors where the two points on a track are so close that the multiple scattering is negligible. The difference between the two centroids, corrected from the track angle given by the drift chambers, has a gaussian distribution (enclosed Figure 16). Assuming the two Micromegas have the same resolution, the standard deviation of this distribution, divided by $\sqrt{2}$, gives the resolution. The spatial resolution, of the order of $65 \mu\text{m}$, is independent of the gain of the chamber (Figure 16). Our Monte-Carlo shows that the resolution is mainly due to the transverse diffusion of the gas. The agreement with the data is obtained with a transverse diffusion of $200 \mu\text{m}$ in the 3 mm drift gap.

6.3 Gas mixture dependence

We have worked with Argon mixed with DME at concentration of 7%, 10% and 15% at a constant gain of 2700, measured on strips, where the efficiency is 99%. We observe a decrease in the cluster size with the DME concentration (Figure 17a) which shows the effect of a decrease in the transverse diffusion. The cluster size decreases from 2.6 at 7% to 2.1 at 15% DME, with an improvement in position resolution (Figure 17b) reaching $55 \mu\text{m}$.

6.4 Track angle dependence

With the second set-up we took data with the rotating chamber in order to estimate the effect on the spatial resolution of the angle of the track on the detector plane.

We came back to the gas mixture of 90% Argon with 10% DME. The drift voltage

was fixed at 1000 Volts and the mesh voltage at 370 Volts which corresponds to the beginning of the plateau efficiency. During this run we could not solve a tiny leakage in the gas circulation. As a consequence the efficiency is not so good as previously, limited at 95%, but stays at this level for any track angle up to 35 degrees.

The spatial resolution of the rotating Micromegas is determined with the two Micromegas doublets used as telescope. The interpolated point is obtained from the doublet points with a precision of $50 \mu\text{m}$. Convolved with the $18 \mu\text{m}$ due to multiple scattering, we get the error of the expected point of the track in the rotating detector. The standard deviation of the difference between the centroid of the cluster and the interpolated point gives the spatial resolution, after deconvolution of the expected error.

The Figure 18 shows a strong dependence of the position resolution with the track angle. It fits well with a convolution of two terms: a constant term, $71 \mu\text{m}$, which corresponds to the resolution at normal incidence; a second term, $195 \mu\text{m}$ per mm, proportional to the length of the piece of track through the conversion gap projected on the detector plane, which describes the degradation of the spatial resolution.

7 Tests at high flux

7.1 Laboratory tests

We have carried out first beam tests of a single detector at the Saclay TANDEM facility. This is a Van de Graaf accelerator, which can provide an intense proton beam with kinetic energy up to 20 MeV. The beam intensity can be tuned from 5 to 500 nA. We have observed [9] that the gain of the detector do not saturate up to $10^9/\text{mm}^2/\text{s}$. A fast investigation (80 minutes) was performed, in these last conditions, to test the radiation resistance of the detector. With a gas mixture Ar + 20% DME there was not aging effect up to $50 \text{mC}/\text{mm}^2$. It corresponds to about 30 years for a detector located at 70 cm from the beam pipe of the LHC collider, running at its full luminosity.

Systematic studies in the laboratory, using a high current X-ray generator emitting at 8 KeV, confirm the above result. Figure 19 shows the measured current as a function of the high voltage HV2, for various particle fluxes up to $8 \times 10^6 \text{X-rays}/\text{mm}^2/\text{s}$. A good linearity of all these curves is observed, so again we do not observe any saturation.

The maximum achievable gain, however, decreases with the flux (Figure 20), but still higher than 1000 at flux of $10^7 \text{Hz} / \text{mm}^2$. Which means that, with a good electronics (noise of the order of 1000 electrons) Micromegas can operate with full efficiency at such high fluxes. This effect is under study to understand the origin of this limitation and to improve the result by using other gas mixtures.

Using the same set-up a lot of investigations have shown the radiation resistance of this detector. These results will be published in a subsequent paper. The detector operating with a mixture Ar + 6% Isobutane at a gain of 2500 was irradiated with a 5 mm collimated X-ray beam up to a total charge of $19 \text{mC}/\text{mm}^2$ which is about 10 year LHC operation. Figure 21 show the relative gain of the detector versus the time (11 days test). Again there is not any radiation damage effect.

7.2 Beam tests

We have pursued our study with the goal of adapting Micromegas to experiments projected in the near future, one of them is COMPASS [16]. In the very-forward region of the experiment it requires chambers operating at rates higher than those foreseen of LHC : $10^6/cm^2/s$. To deal with such environment one has to optimize the time resolution of the detector as well as some geometrical parameters. The depth of the amplification gap controls the occupation time of the positive ions. The depth of the drift gap determines the signal width due to the drifting electrons. The limit is set by the need for an efficiency close to unity.

We have tested three Micromegas chambers (2 with 100 μm amplification gap and 1 with 50 μm) at the CERN SPS beam (M2) of 100 GeV/c negative muons at a flux up to $5 \times 10^7/cm^2/s$. We have made the study with an electronic system faster than the preexisting one. It is a standard Lecroy preamplifier called MQS104A having a rise time of 10 ns and the integration time 16 ns. The sensitivity was 25 V/pC and the electronic noise 3000 electrons. However when the chip was mounted on the detector the noise has increased by a factor of two. Although the electronics is not optimized the results obtained show clearly the progress.

In view of the large number of channels foreseen at COMPASS (several tens of thousands), a digital read out was tested. The time of both the leading and the trailing edges of the signal was recorded with multihit TDC's. Thus the width of each signal is known and allows to reject the noise which has a very small width. The width is also used to improve the spatial resolution since it is correlated with the charge.

Figure 22 shows the efficiency as a function of the applied voltage in the amplification gap. It is difficult to reach a plateau. As it has already pointed out this electronics is too slow for the signal induced by the electrons in the avalanche (1ns) and too fast for the signal induced by the ion motion hence the loss in gain. To improve the result one has to increase the integration time constant of the preamplifier to a value of 30 ns and decrease the noise to about 1000 electrons.

We have measured the time jitters of the electronic signal with respect to the trigger time. With Argon + Cyclohexane mixture the time resolution is only 20 ns. By adding CF_4 the time resolution is improving and it is about 5 ns with 30% CF_4 . The time jitters will be further reduced by using pure CF_4 as carrier gas and by employing very-fast electronics.

8 Micromegas in a magnetic field environment

The performances of Micromegas have also been studied in a magnetic field up to 1.3 Tesla. We have installed two Micromegas chambers in the experimental set-up of TOSCA [11], prototype of a spectrometer inside a dipole magnet. The test was performed in the CERN-PS pions beam T9. The two Micromegas chambers were filled with 90% of Argon and 10% of Isobutane. Silicon strips detectors have been used to reconstruct with high resolution the extrapolated point of the track in Micromegas.

Preliminary results indicate that the amplification gain is not affected by the magnetic

field. The Lorentz angle is found at the expected value, 15 degrees at 1 Tesla. The resolution with the gas used is $80 \mu\text{m}$ for normal incident tracks without magnetic field. At 1 Tesla, it grows up to $110 \mu\text{m}$ due to the Lorentz angle. Turning the detector to compensate this angle, the resolution is restored to about $80 \mu\text{m}$. So, if there is a degradation due to the magnetic field, it is small compare to $80 \mu\text{m}$.

9 Conclusion

Major steps have recently been made in the development of a very-high rate, high precision gaseous detector. We have tested several $15 \times 15\text{cm}^2$ Micromegas detectors in intense particle beams. First results indicate good behaviour of the detector. After a total of 3 month tests in hard radiation environemnt the detector was stable and reliable.

The operation of several Micromegas prototypes set up in various beam conditions has shed light on the rate capability, the long-term stability, the space resolution and the efficiency for minimum ionising particles. We give a list of our major results :

- With heavily ionizing particles (10 MeV protons) the detector was able to operate at very high fluxes, up to 2×10^9 particles/ mm^2/s without saturation of the amplification factor. We have found it is possible to work under conditions of total protection of the detector and of the electronics from occasional sparks.
- Preliminary radiation dammage tests have shown a rather good resistance of the detector. They have been performed at very high particle rate. Further detailed tests are in preparation to measure the radiation resistance of the detector.
- Full efficiency with large plateau are obtained with several gas mixtures. With 1.2 mm conversion gap the efficiency was 95%. With an optimisation of the electronics larger plateau are expected.
- A first investigation of the space resolution shows that one can achieve a precision of about $50 \mu\text{m}$ with strip pitch of $317 \mu\text{m}$. It is limited by the diffusion coefficient of the gas mixture and strip width. Better resolution can be obtained by using gases having lower diffusion coefficient and narrow anode strips.
- Gas mixtures with CF_4 exhibit high gas gains and good drift and diffusion properties.
- The time resolution was measured to be 5 ns. With a better choice of the gas mixture and faster current preamplifiers a time resolution of about 1 ns is expected.
- Fast signals with 1ns rise time have been obtained reflecting the fast movement of the electrons during the avalanche development. The way is may-be open to operate high resolution detectors in the Ghz region able to cope with intense radiation environments.

10 Prospects

(i) Time resolution

The time resolution (5 ns) obtained, limited by the preamplifier rise, can be improved by using faster preamplifiers. Another way to improve the result is the

use of CF_4 gas mixtures which increase the electron drift velocity by a significant factor. So, our objective is to achieve, in the near future, time resolution of 1 ns.

(ii) Spatial resolution

The use of CF_4 mixture also constitute a key point to improve the spatial resolution. As it has been shown, the obtained spatial resolution (50 micron) was limited by the transverse electron diffusion in the conversion gap. By using CF_4 mixtures the diffusion coefficient can decrease by a factor of three. At the same time the number of primary electrons, produced by the incident particle in the drift gap, is 3-4 times higher in this mixture, which improves the accuracy of the charge interpolation between anode strips.

The decrease of the diffusion coefficient must, however, to come with a decrease of the anode pitch in order to keep the strip multiplicity, per incident particle, at the order of 2, which is the optimal value for efficient charge interpolation. Monte Carlo simulations show that spatial resolution of about 10 microns is under reach with anode pitch of 100 micron. A detector with optimised pitch, electronics and gas mixture is under construction to explore the ultimate spatial resolution of the detector.

(iii) Technical developments

Micromegas chambers of size $30 \times 40 \text{ cm}^2$ are under construction for the high rate Compass experiment. First tests look promising.

To decrease the material budget, thin substrates in epoxy or kapton will be tested.

The two dimensional read-out will be investigated with 2D strips or pads.

A more systematic study will be pursued to decrease both the conversion and amplification gap.

We believe that those developments can lead, in the near future, to a new generation of simple, cheap, high resolution, position sensitive detectors permitting high precision tracking or vertexing close to the interaction region, in very high-rate environments.

(iv) Electronics

Although the required electronics depend on the experiment, we would like to develop a very-fast one with band width at the Ghz range. The aim is to catch the full electron signal which is available in MICROMEGAS detector. Using such fast electronics the single electron response of the detector will be explored in the near future in order to evaluate the use of Micromegas in a TPC structure. We are also planning to use it in a photodetector configuration combined with adequate photocathodes compatible with gaseous detectors. Such a photodetector, based on the MICROMEGAS technique, can be used for efficient Cherenkov detection as a basic element of RICH counter or the Hadron Blind Detector [17].

11 Request from CERN for 1999-2000

The funding is fully supported by home Institutes. We would like to request on the CERN infra-structure :

- (i) five weeks test beam, per year, at : SPS (2 weeks) and PS (3 weeks)
- (ii) computing time and disk space on the central CERN computers
- (iii) one office space for our collaboration

References

- [1] Y. Giomataris, Ph. Rebourgeard, J.P. Robert and G. Charpak Nucl. Instr. Meth. A376(1996)29-35.
- [2] G. Charpak, R. Bouclier, T.Bressani, J. Favier and C. Zupancic, Nucl. Instr. Meth. 62(1968)235
- [3] A. Oed, Nucl. Instr. Meth. A263(1988)351
- [4] F. Angelini, R. Bellazzini, A. Brez, M.M. Massai, G. Spandre and M.R. Torquati, Nucl. Instr. Meth. A283(1989)69
- [5] R. Bouclier, J.J. Florent, J. Gauden, G. Million, A. Pasta, L. Ropelewski, F. Sauli and L. I Shekhtman, Nucl. Instr. Meth. A323(1992)236.
- [6] S.F. Biagi, J.N. Jackson, T.J Jones and S. Taylor, Nucl. Instr. Meth. A323(1992)258
- [7] G. Charpak, I. Crotty, Y. Giomataris, L. Roppelewski and C. Williams, Nucl. Instr. Meth. A346(1994)506
- [8] E. Roderburg et al., Nucl. Instr. Meth. A323(1992)140
- [9] G. Charpak et al., NIMA412(1998)47.
- [10] V. Peskov, B.D. Ramsey and P. Fonte, Int. Conf. on Position Sensitive Detectors (Manchester, 9-13 Sept. 1996).
- [11] Letter of Intent, A High Sensitivity Short Baseline Experiment to Search for $\nu_\mu \rightarrow \nu_\tau$ Oscillation, CERN-SPSC/97-5.
- [12] S.F. Biagi, NIM A273 [1988] p533 and NIM A283 [1989] p716, MAGBOLTZ Source Code.
- [13] Results from beam tests, to be published.
- [14] CMS Letter of intent, CERN/LHCC 92-3,1992
- [15] GARFIELD CERN program library W5050
- [16] CERN/SPSLC 96-14 SPLSLC/P297 and CERN/SPSLC 96-30 SPLSLC/P297 add.1.
- [17] Y. Giomataris and G. Charpak, Nucl. Instr. Meth. A310(1991)589

MICROME GAS

Micro Mesh Gaseous Structure

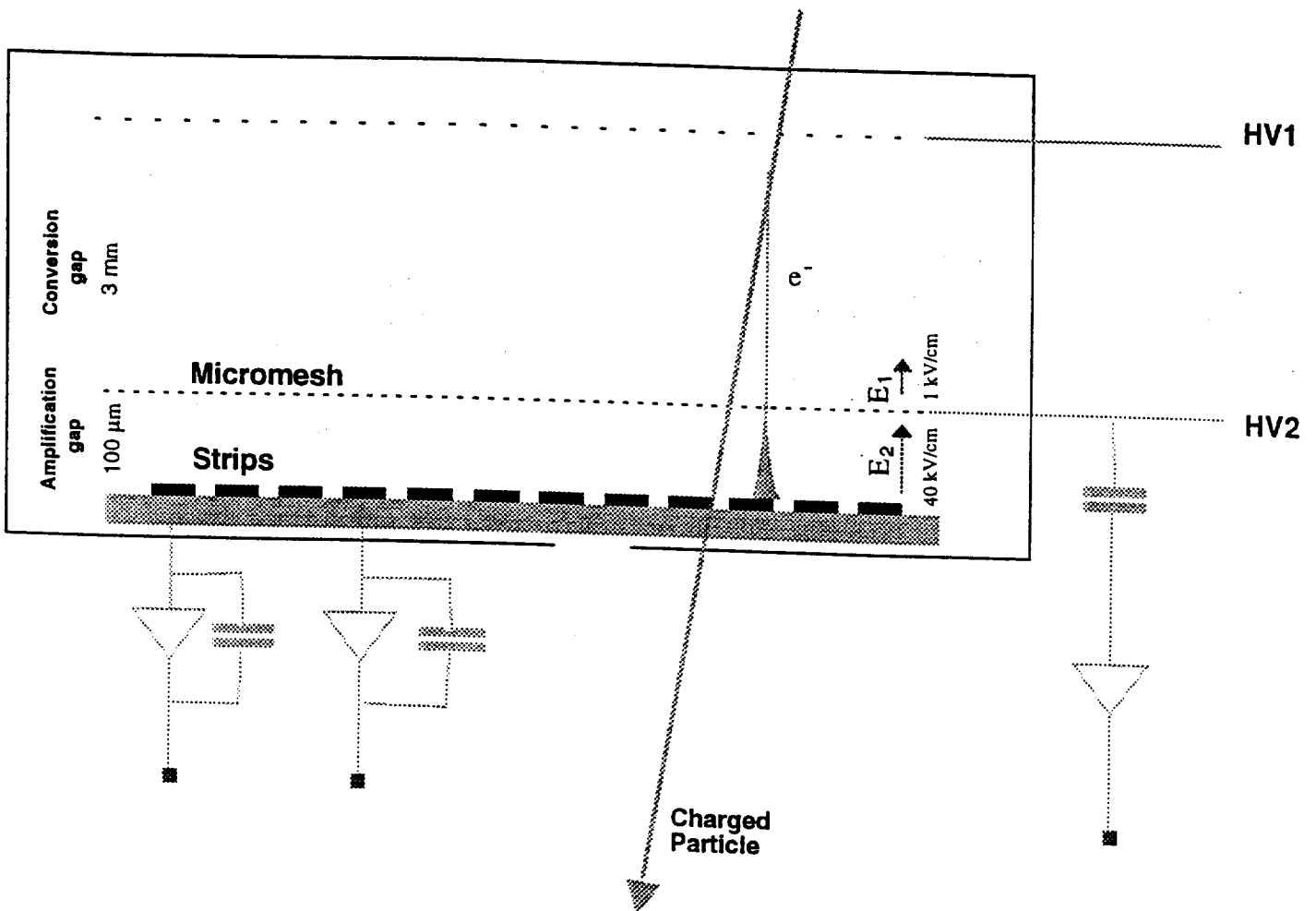


Fig. 1

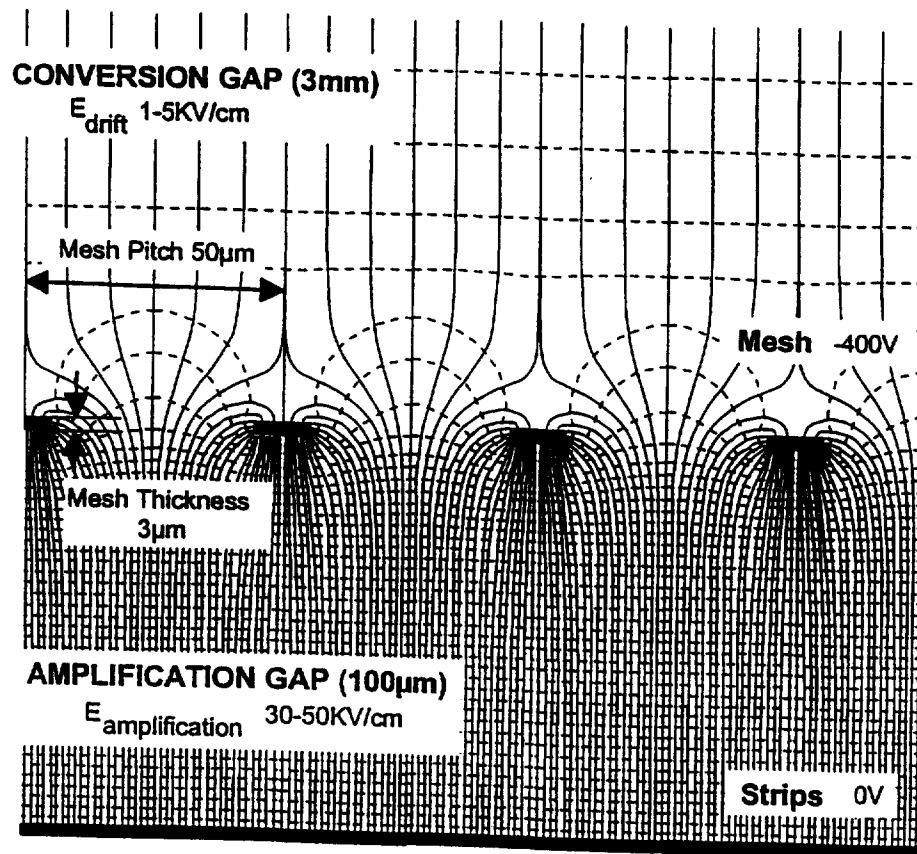


Fig. 2

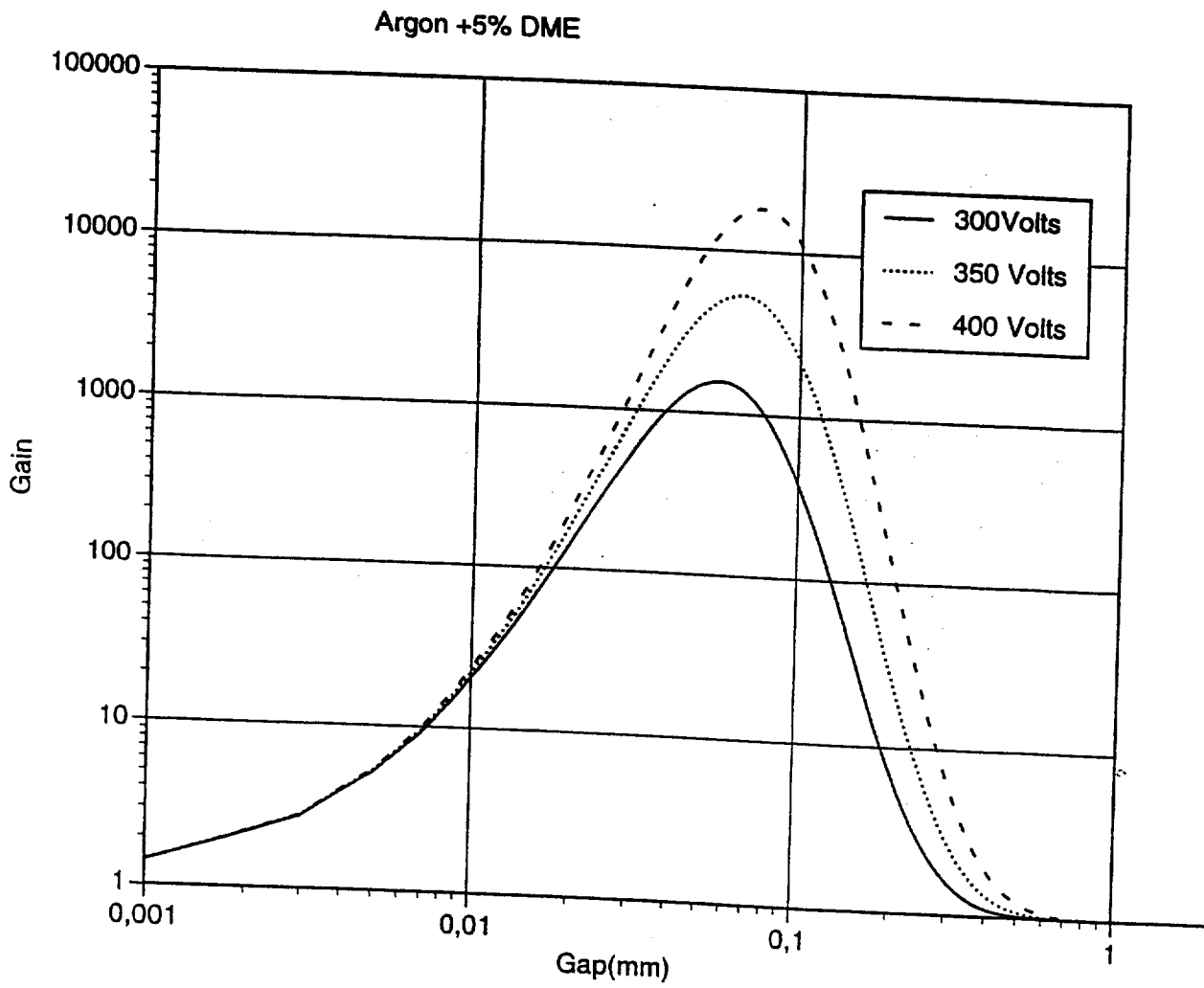


Fig. 3

Fe⁵⁵
Ar+10% Isobutane

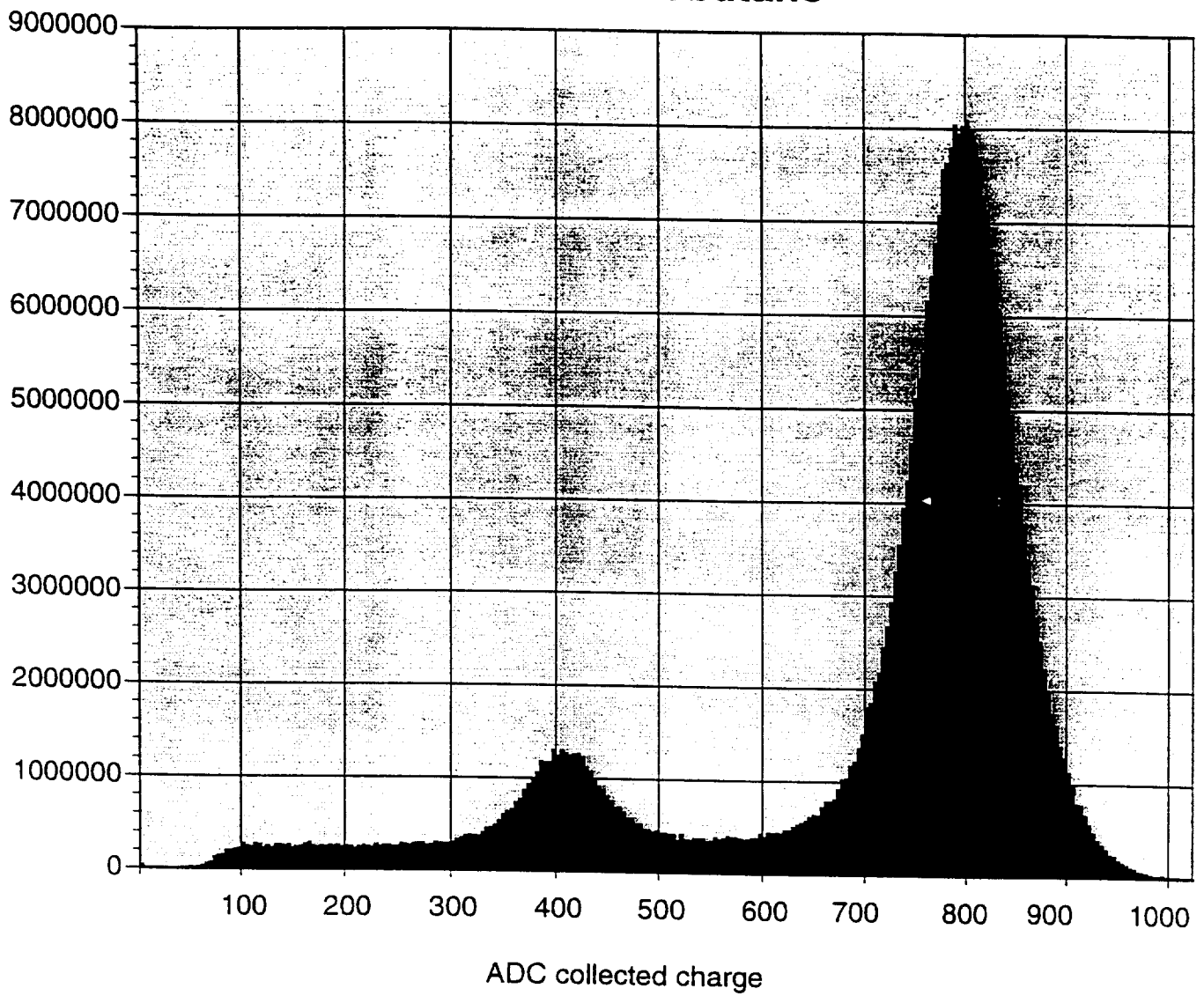


Fig. 4

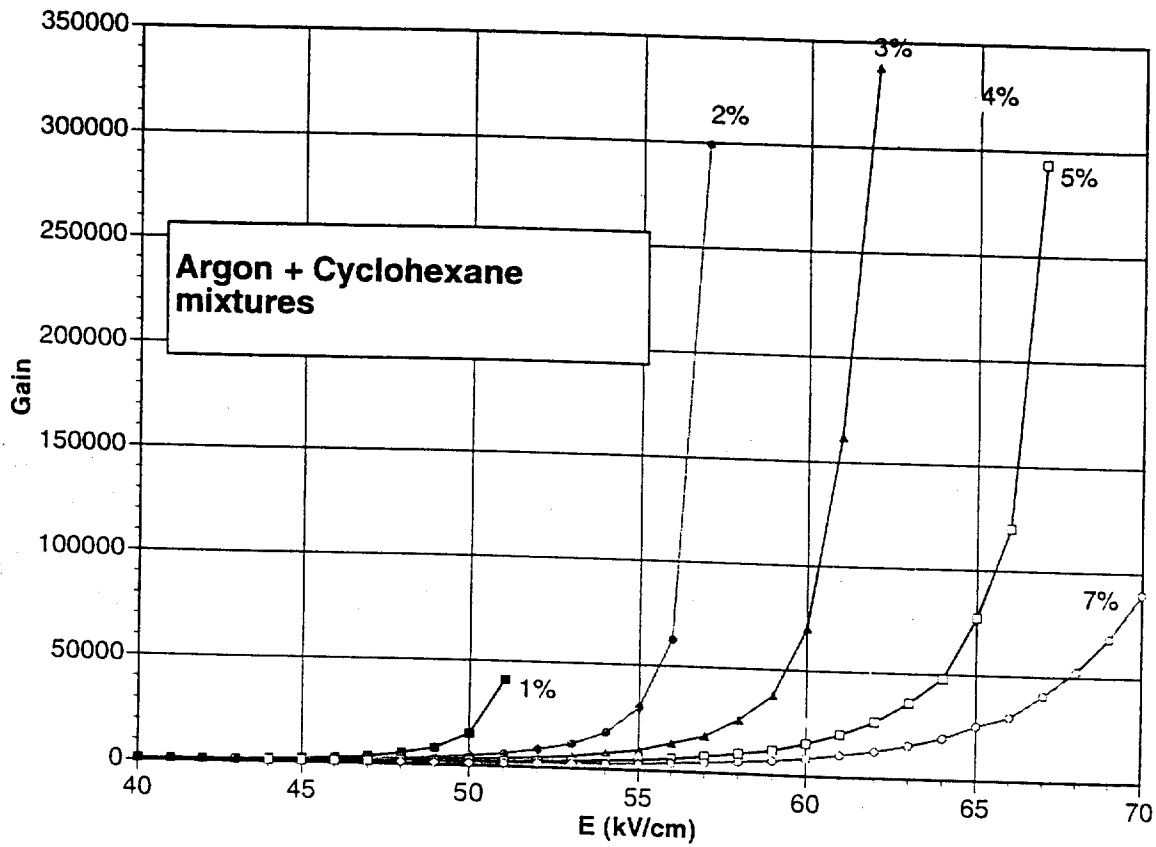


Fig. 5

CF4 + 6,4 % cyclohexane
gene X 20 kV 1 mA

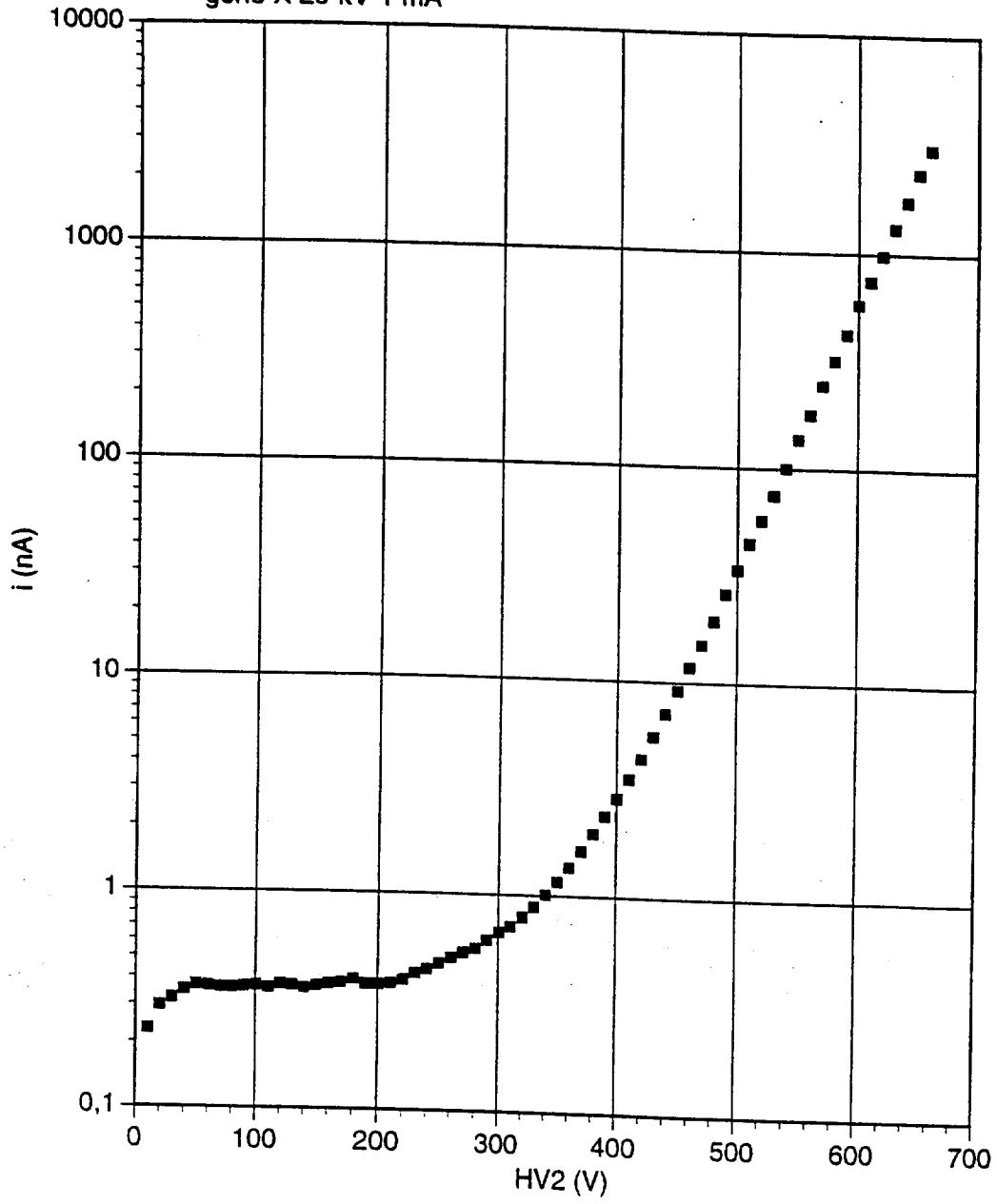


Fig. 6

Ar+10% Isobutane

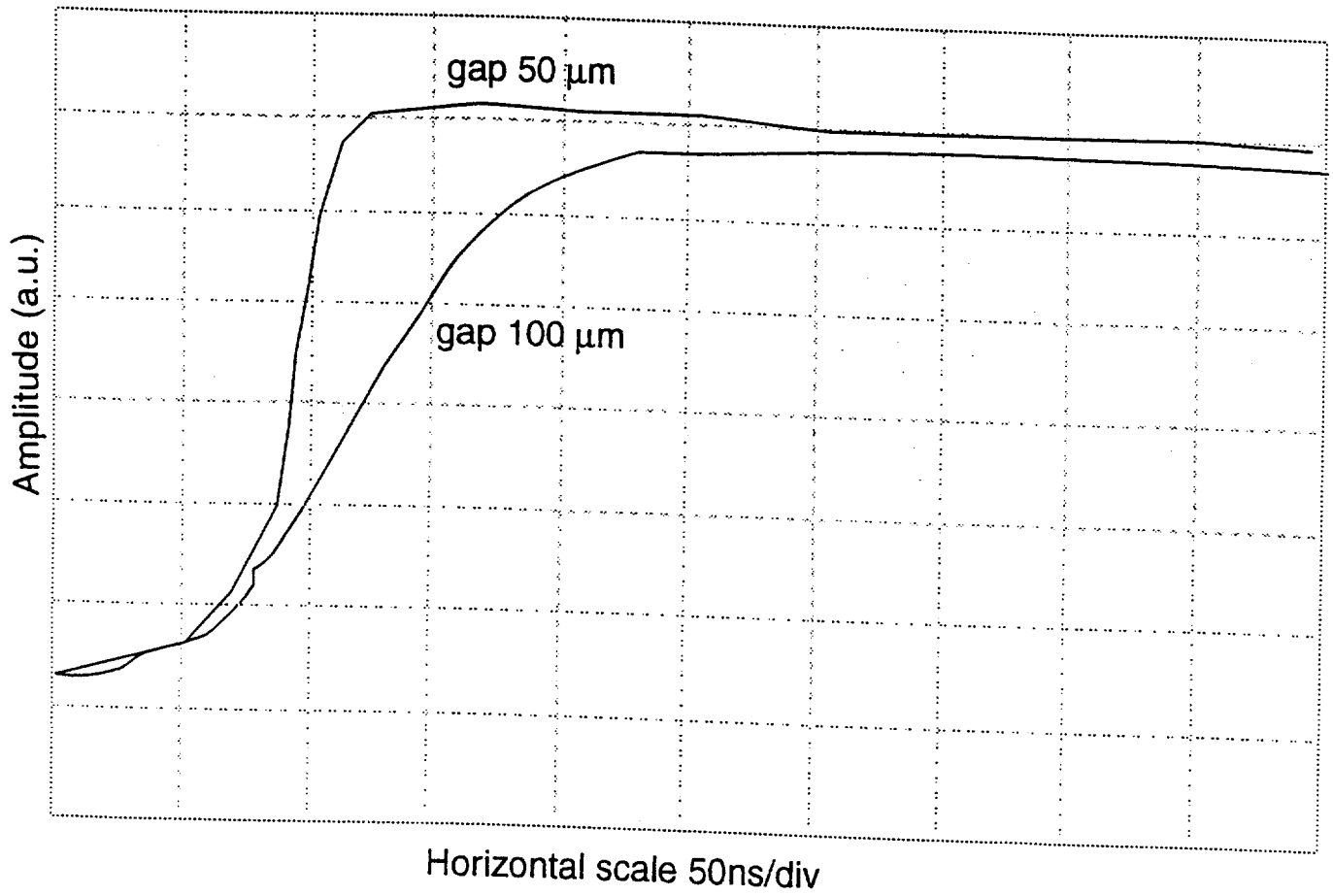


Fig. 7

INDUCTION Time Pattern

- Development of avalanche
 - Electron current < velocity $v_e = 10 \text{ cm}/\mu\text{s}$
 - Induced Charge < Drift over $1/\alpha$
- After Electron collection
 - Ion current < velocity $v_i = 0.1 \text{ cm}/\mu\text{s}$
 - Induced Charge < Drift over d_{amp}

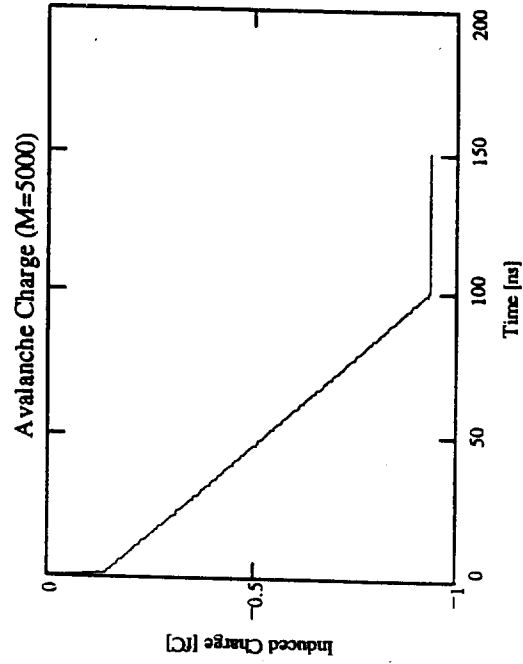
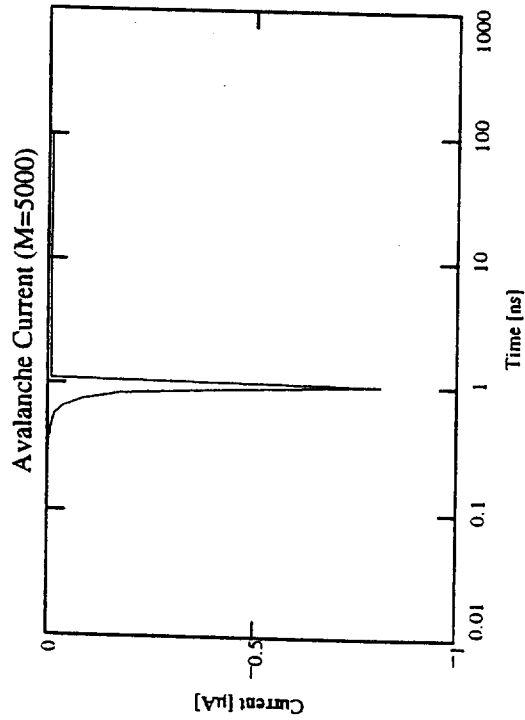


Fig. 8

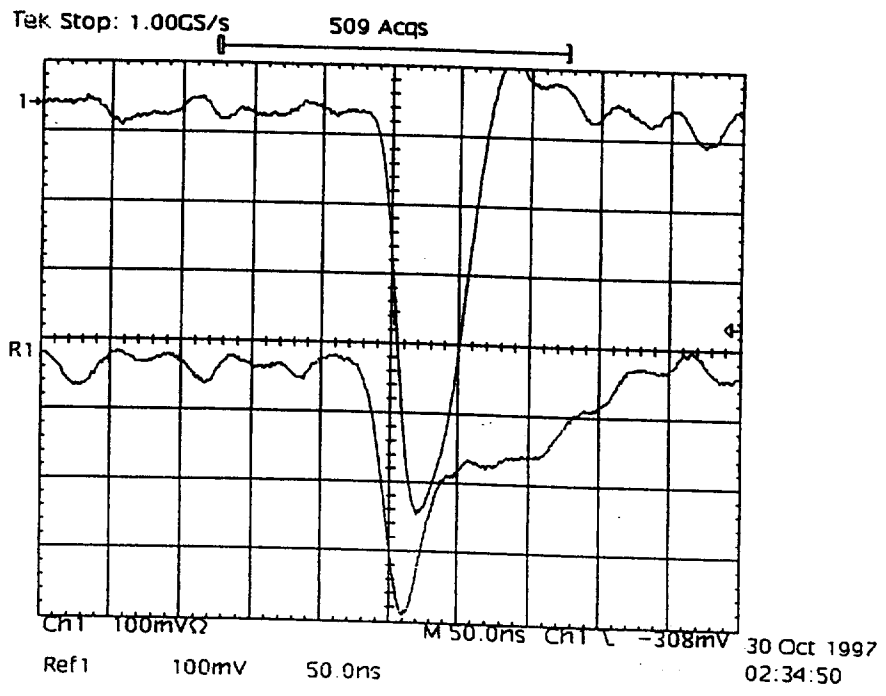


Fig. 9

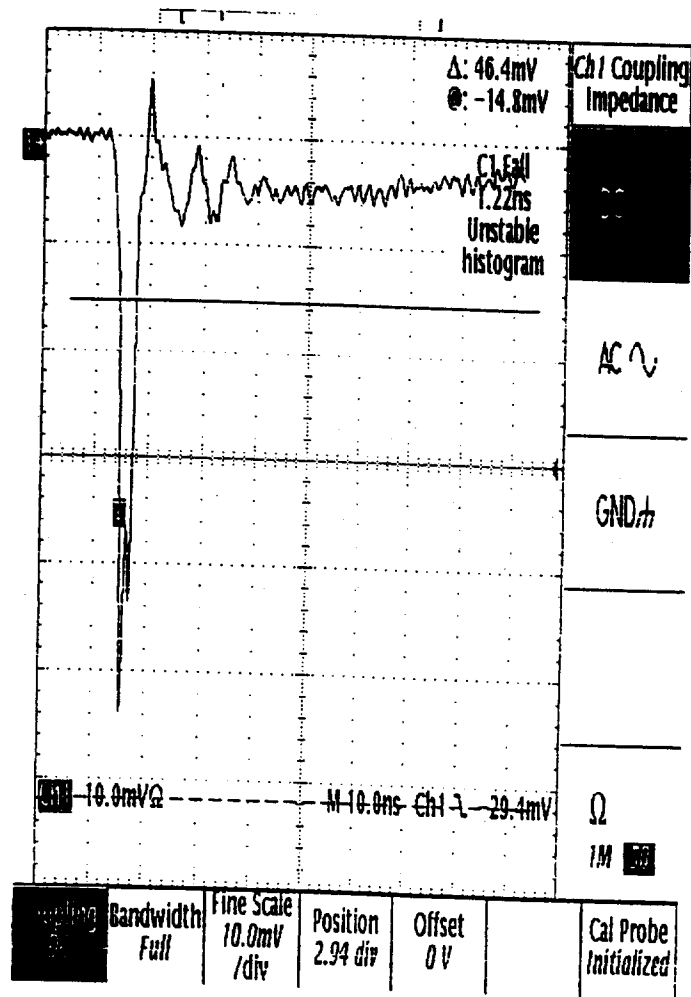


Fig. 10

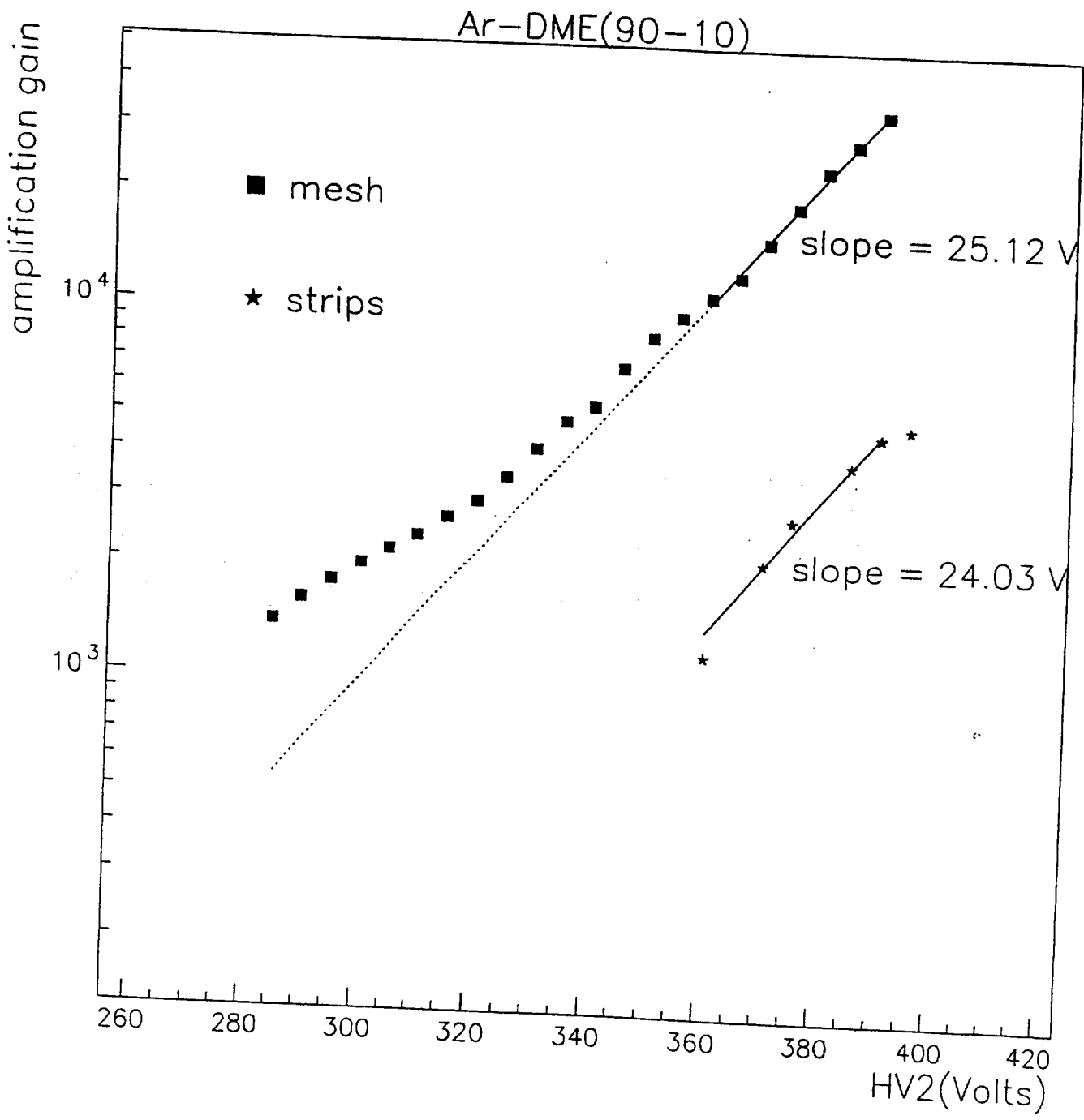


Fig. 11

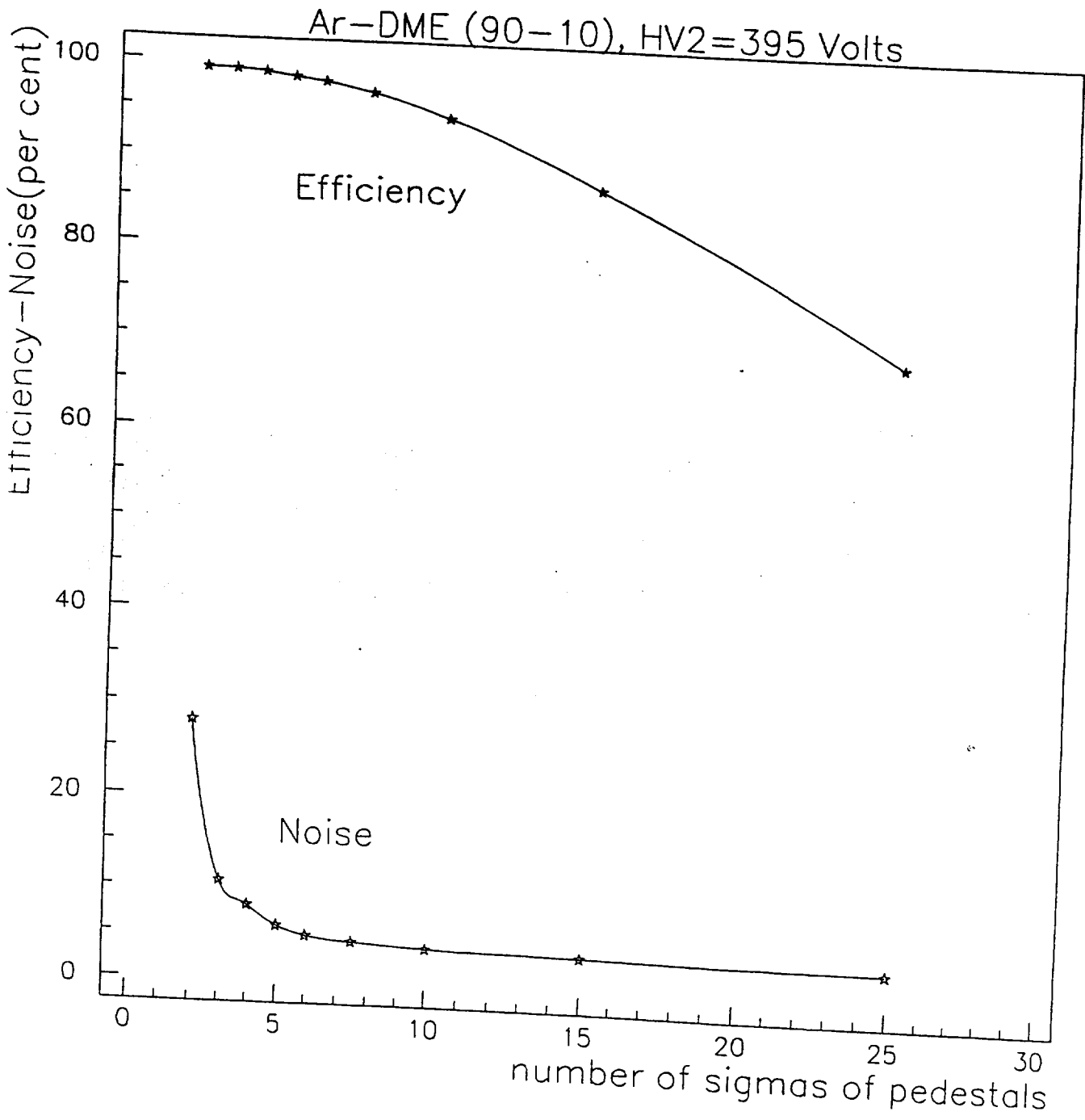


Fig. 12

Ar-DME(90-10)

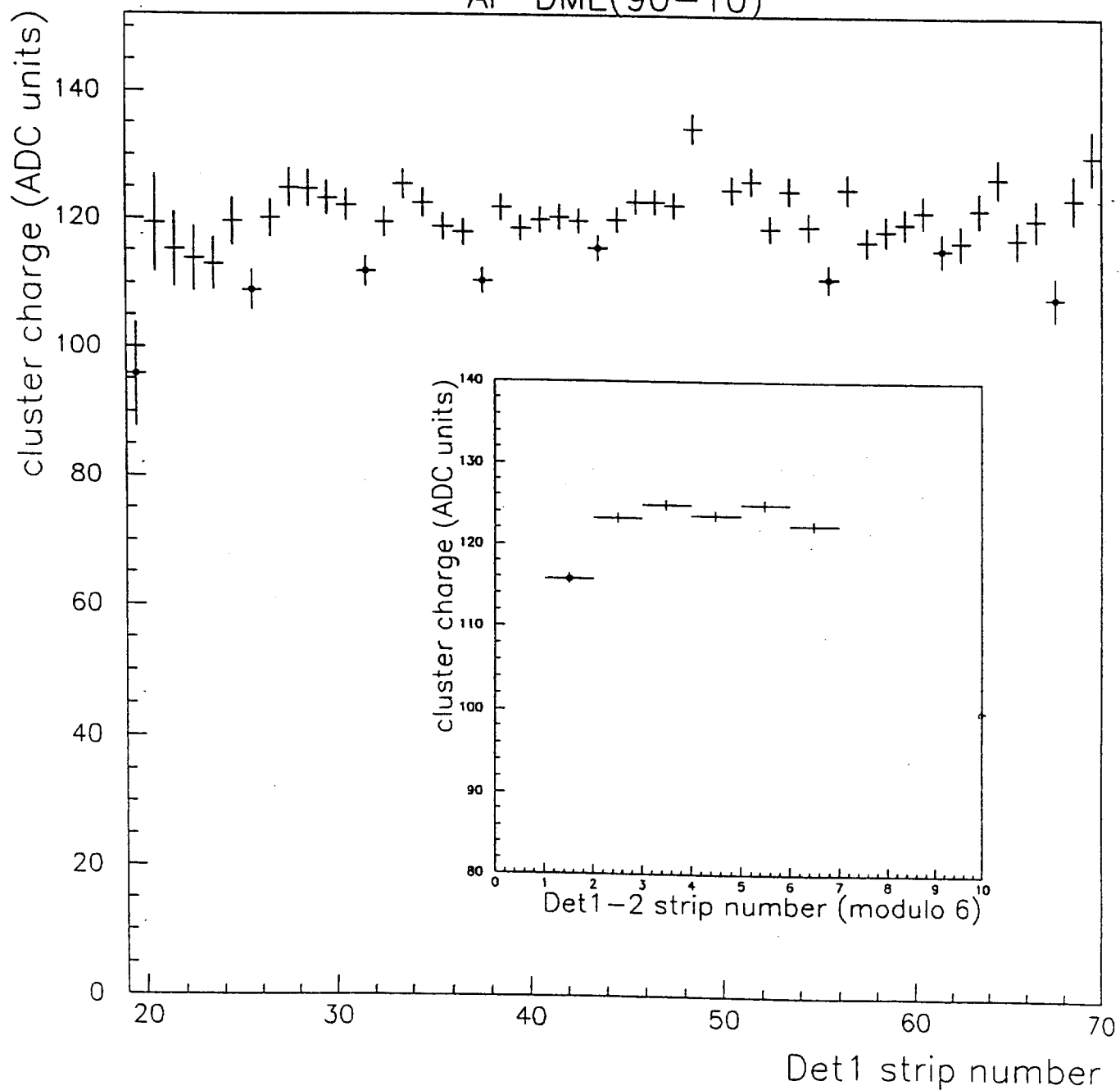


Fig. 13

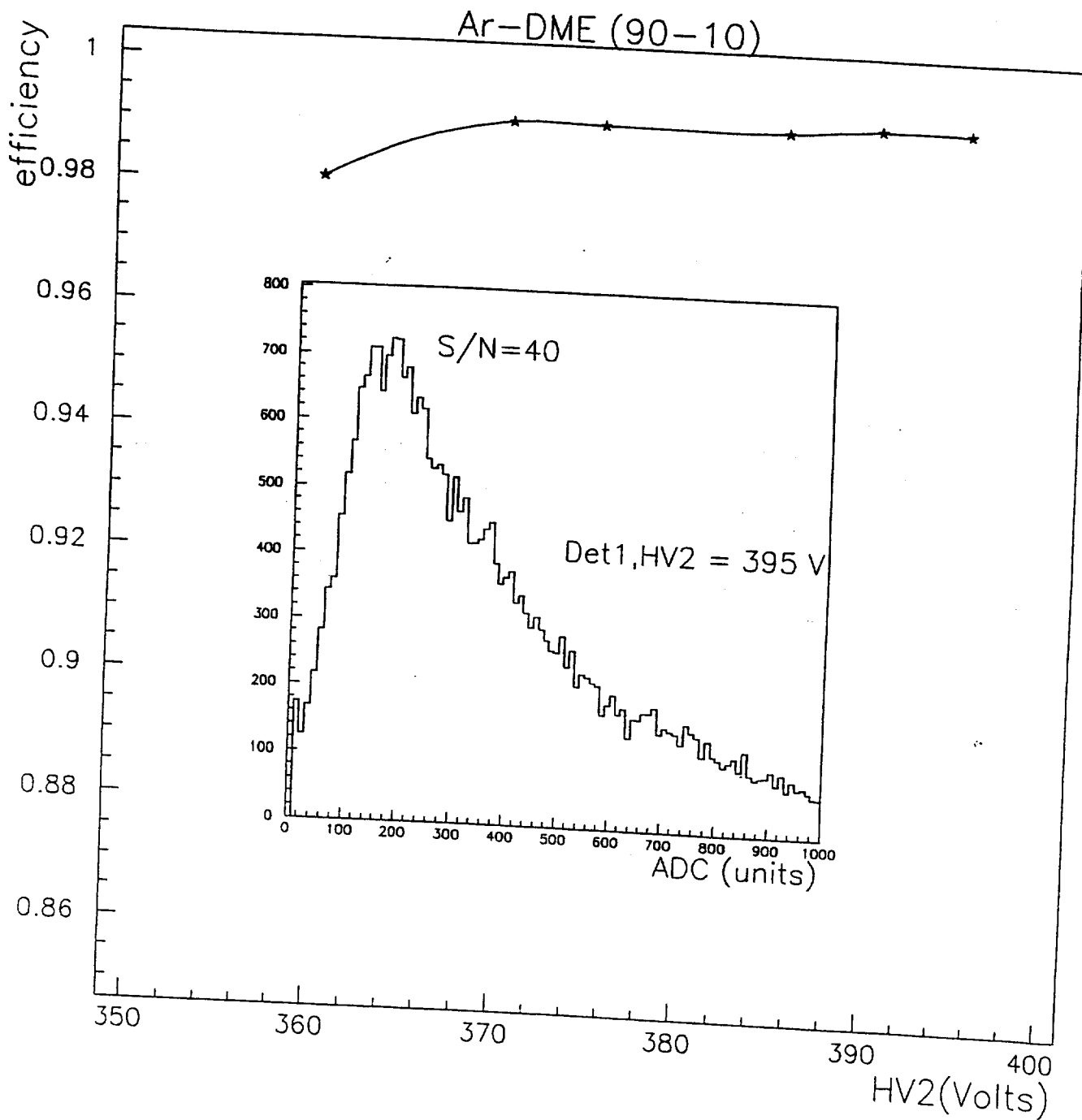


Fig. 14

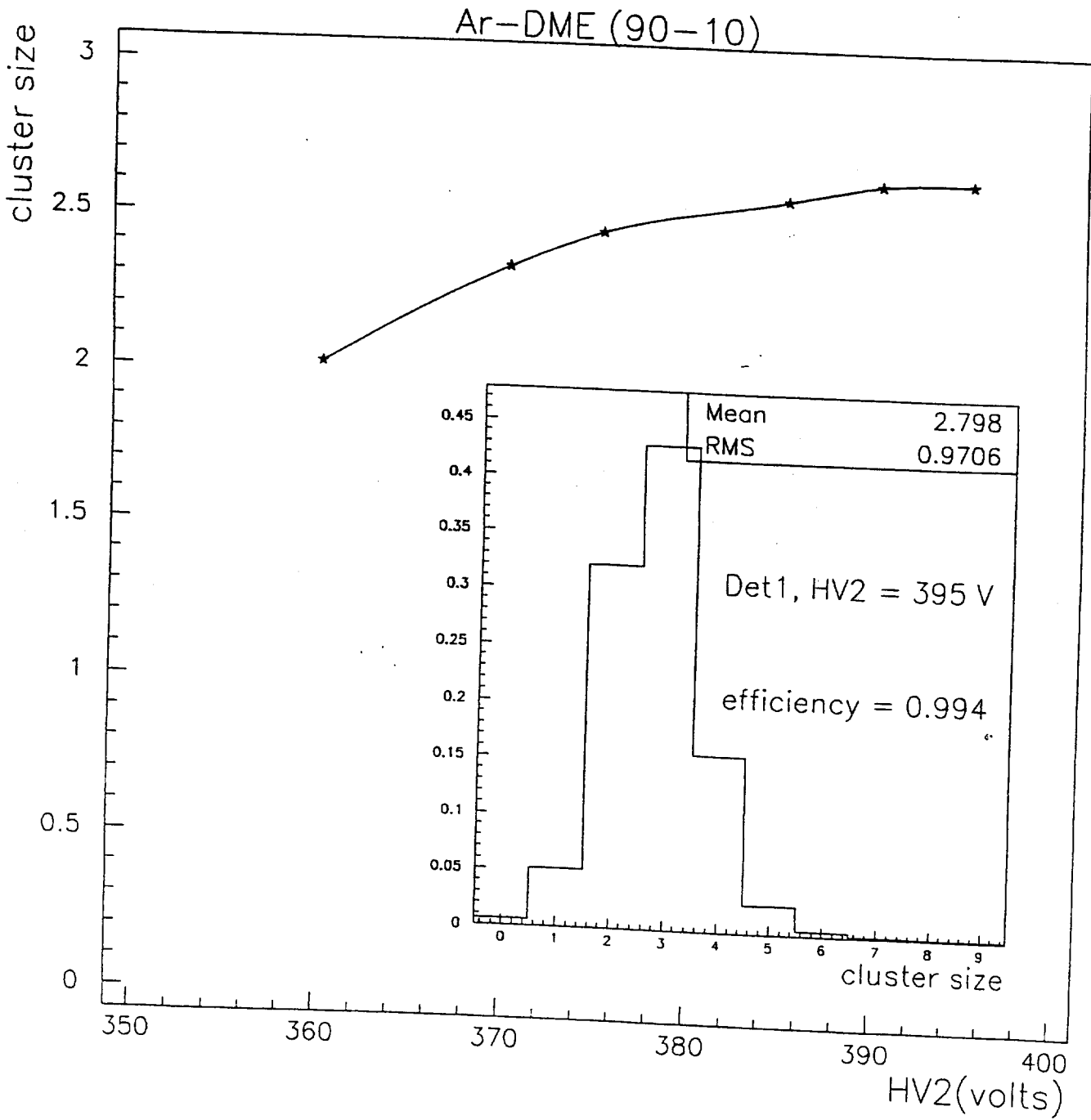


Fig. 15

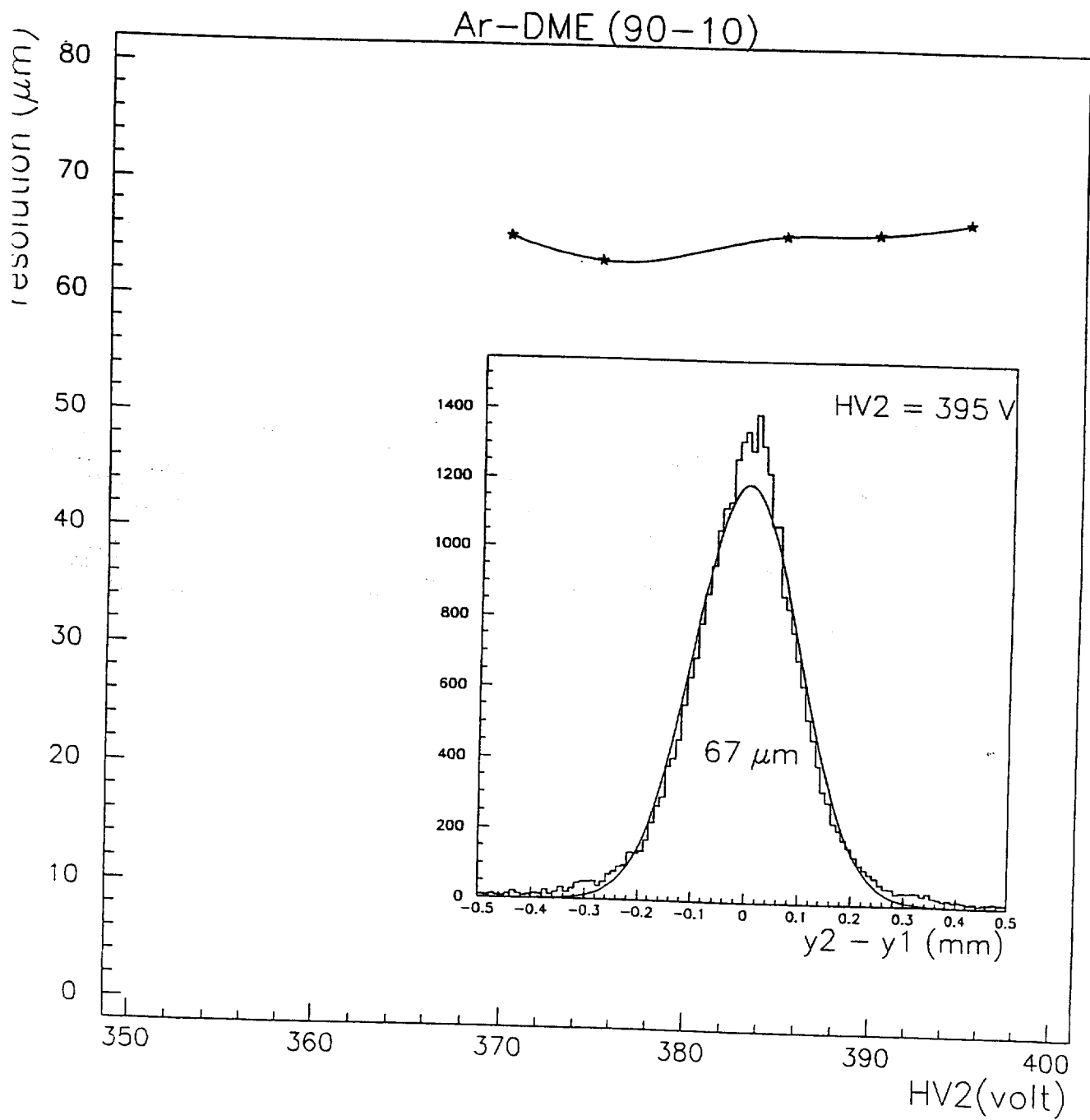


Fig. 16

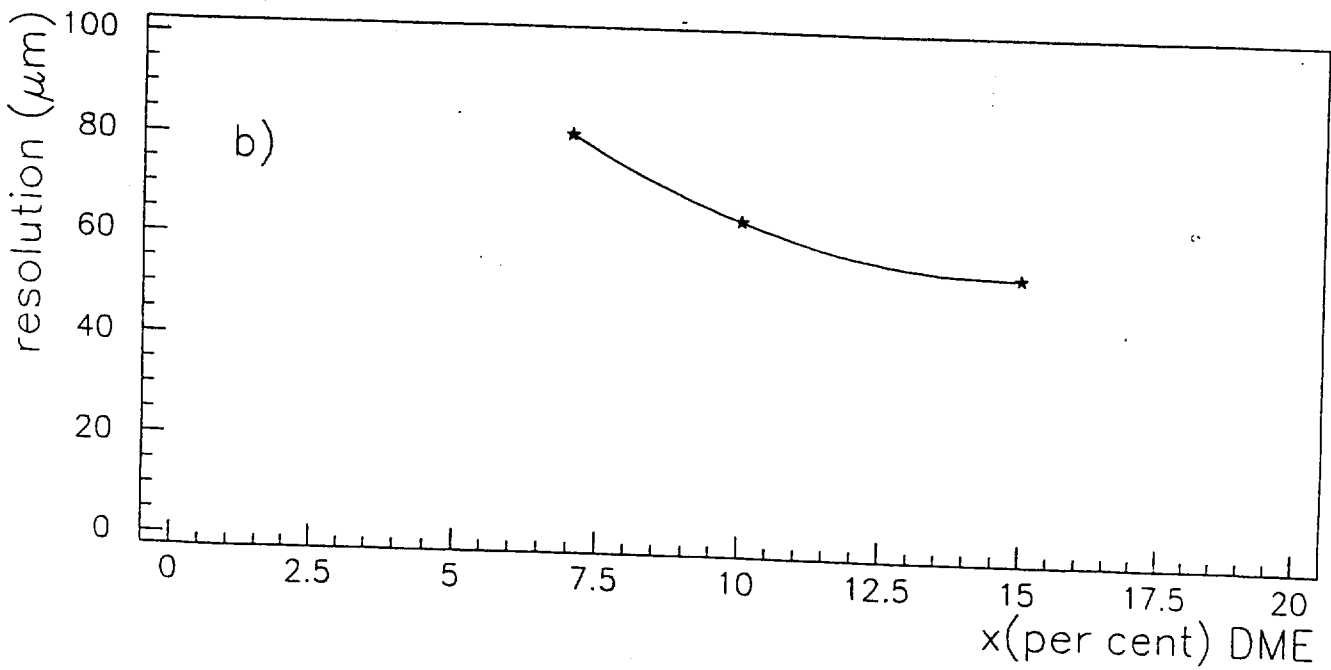
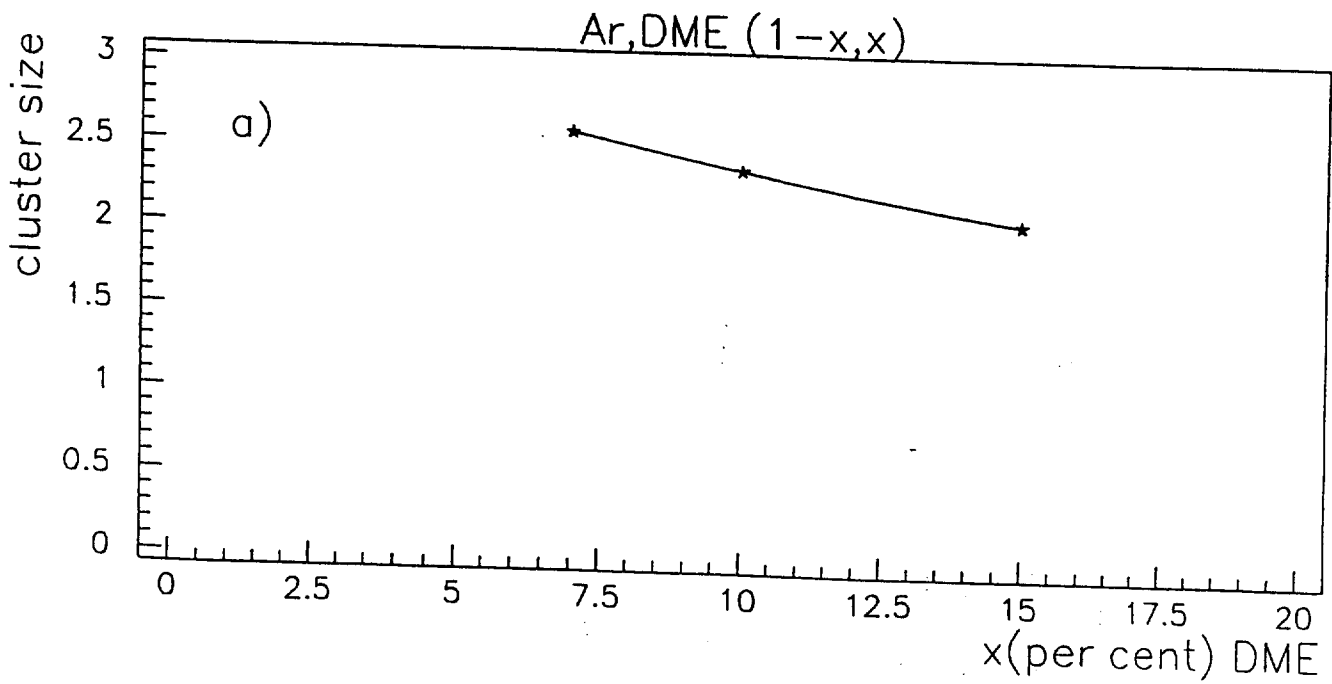


Fig. 17

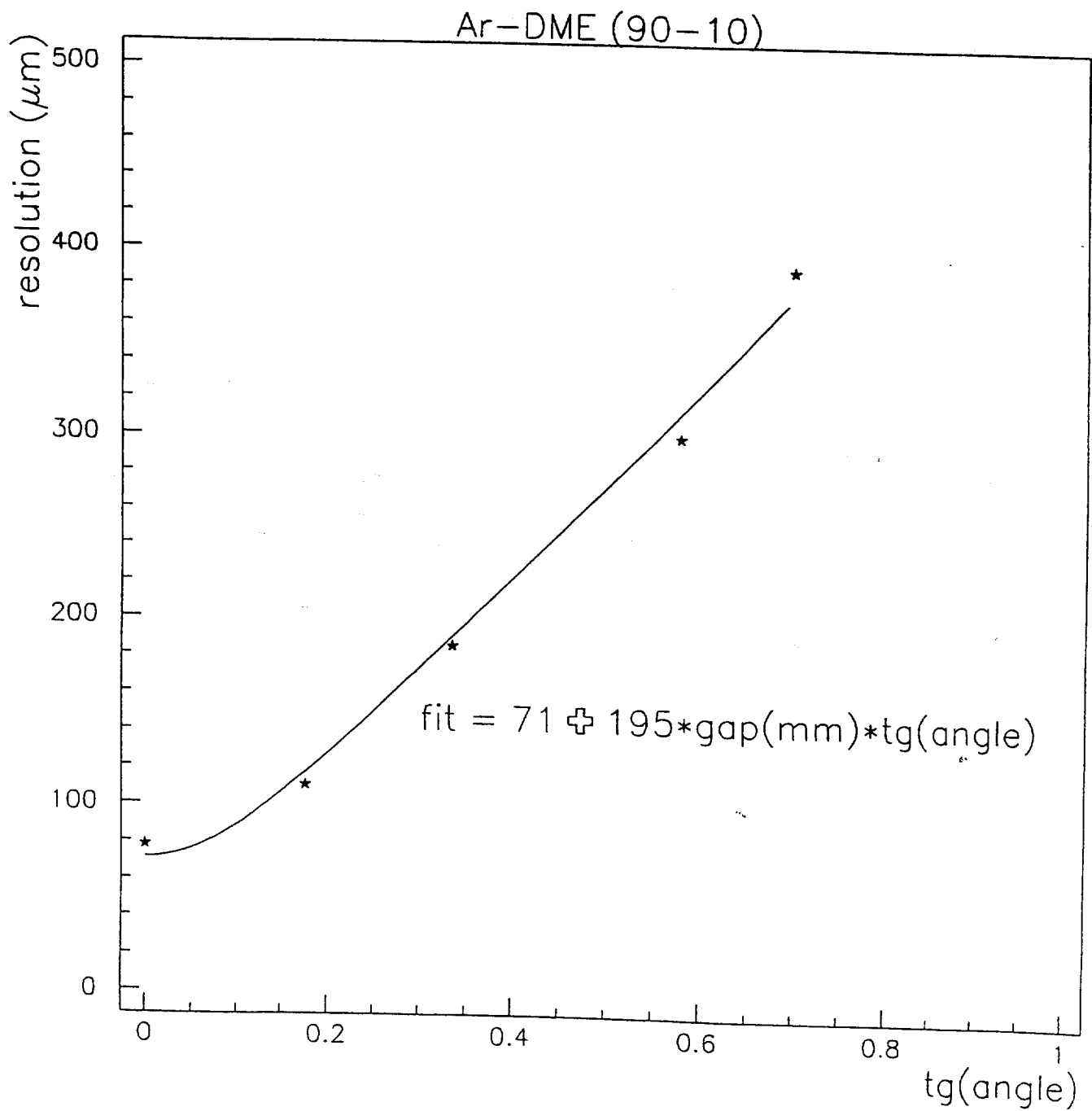


Fig. 18

Argon + 6,6 % isobutane
gene X 20 kV

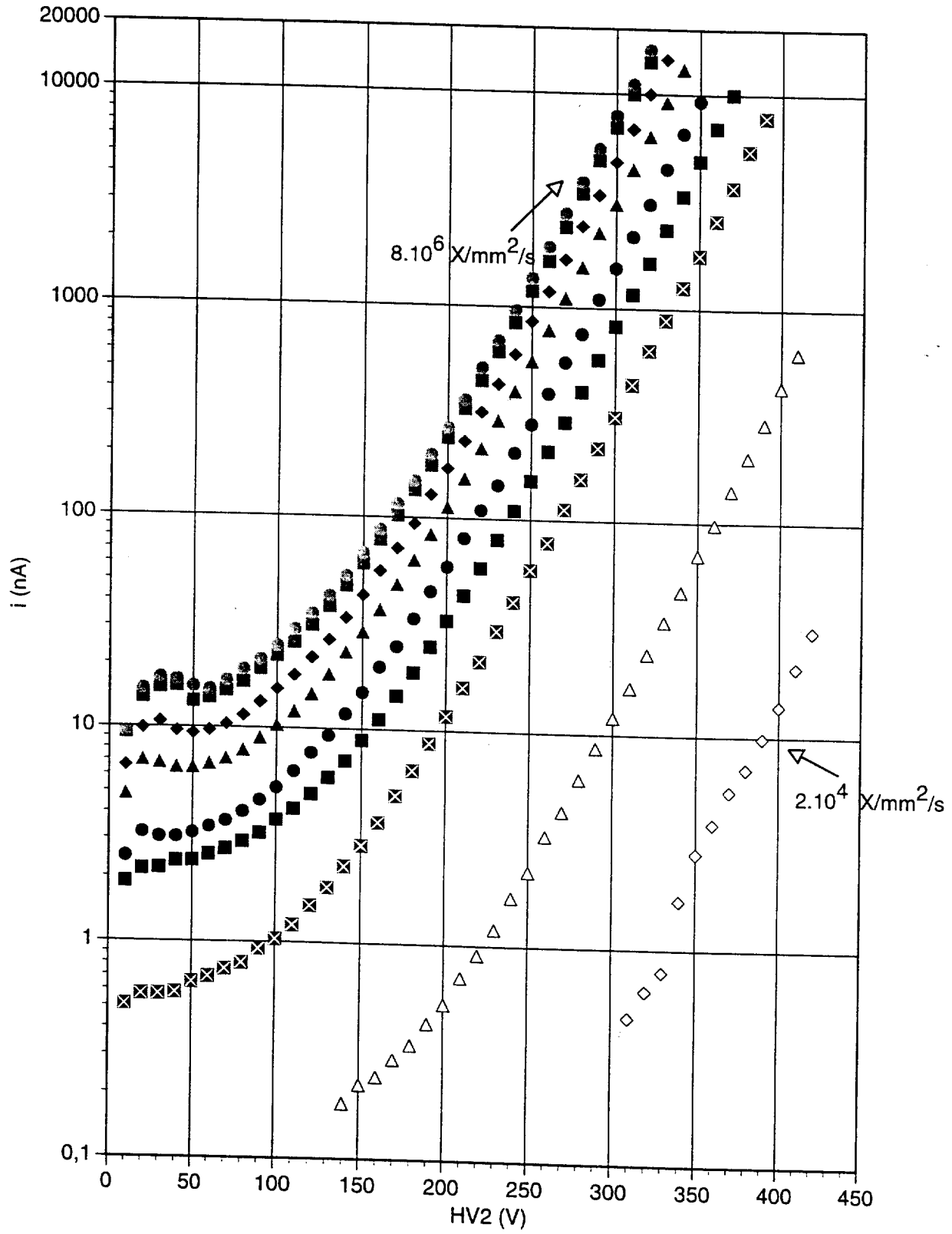


Fig. 19

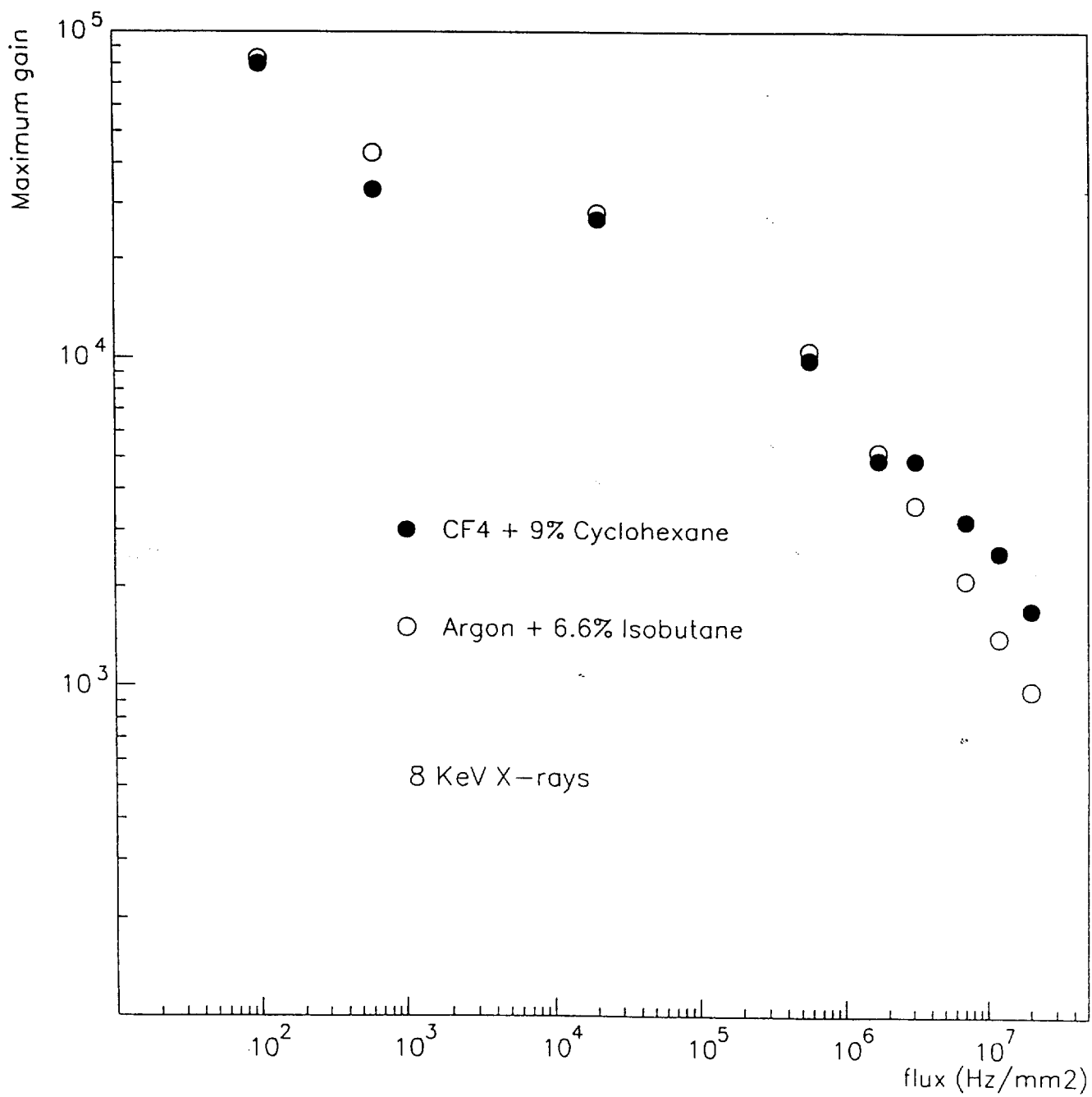


Fig 20

Argon-Isobutane 6%

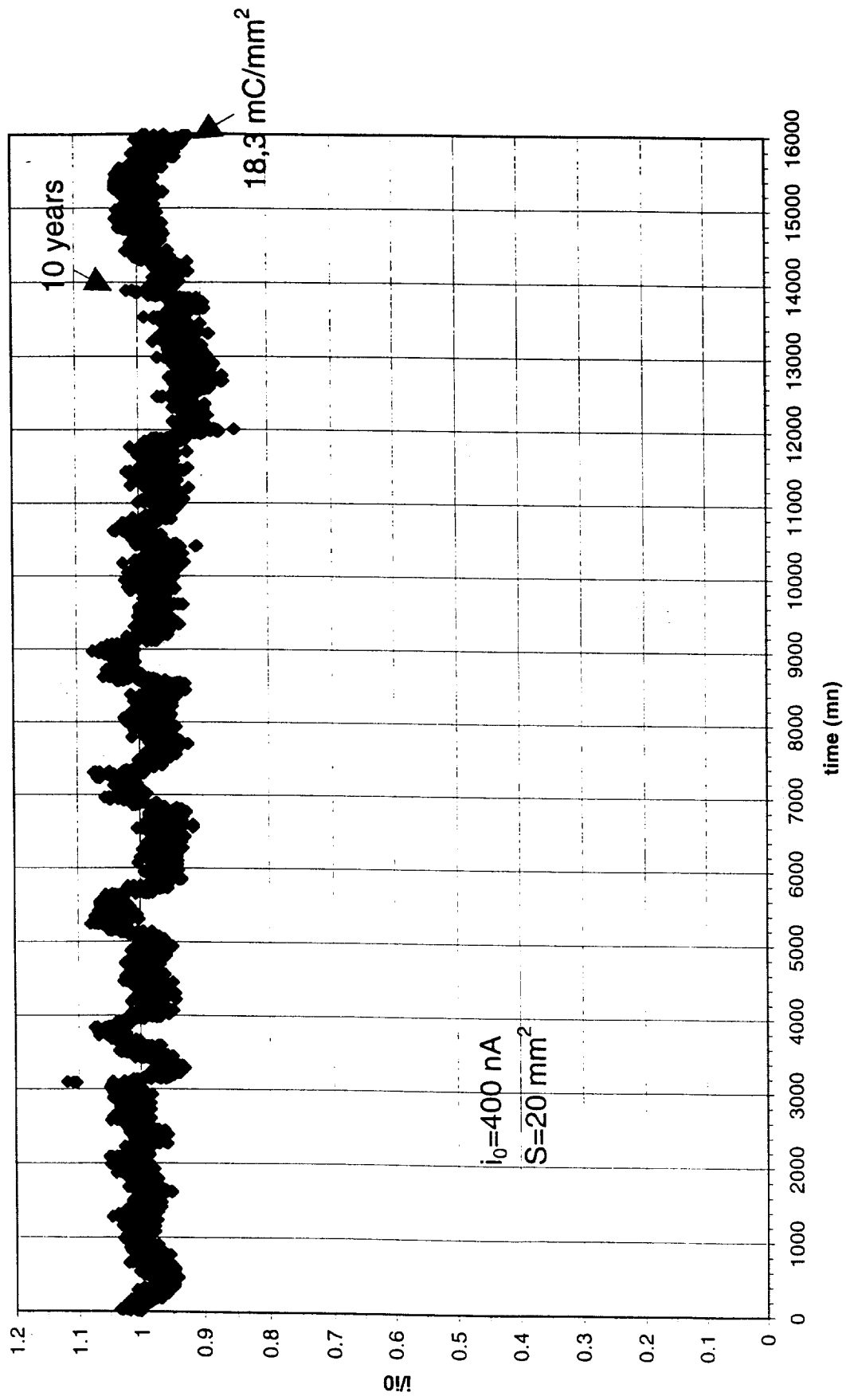


Fig 21

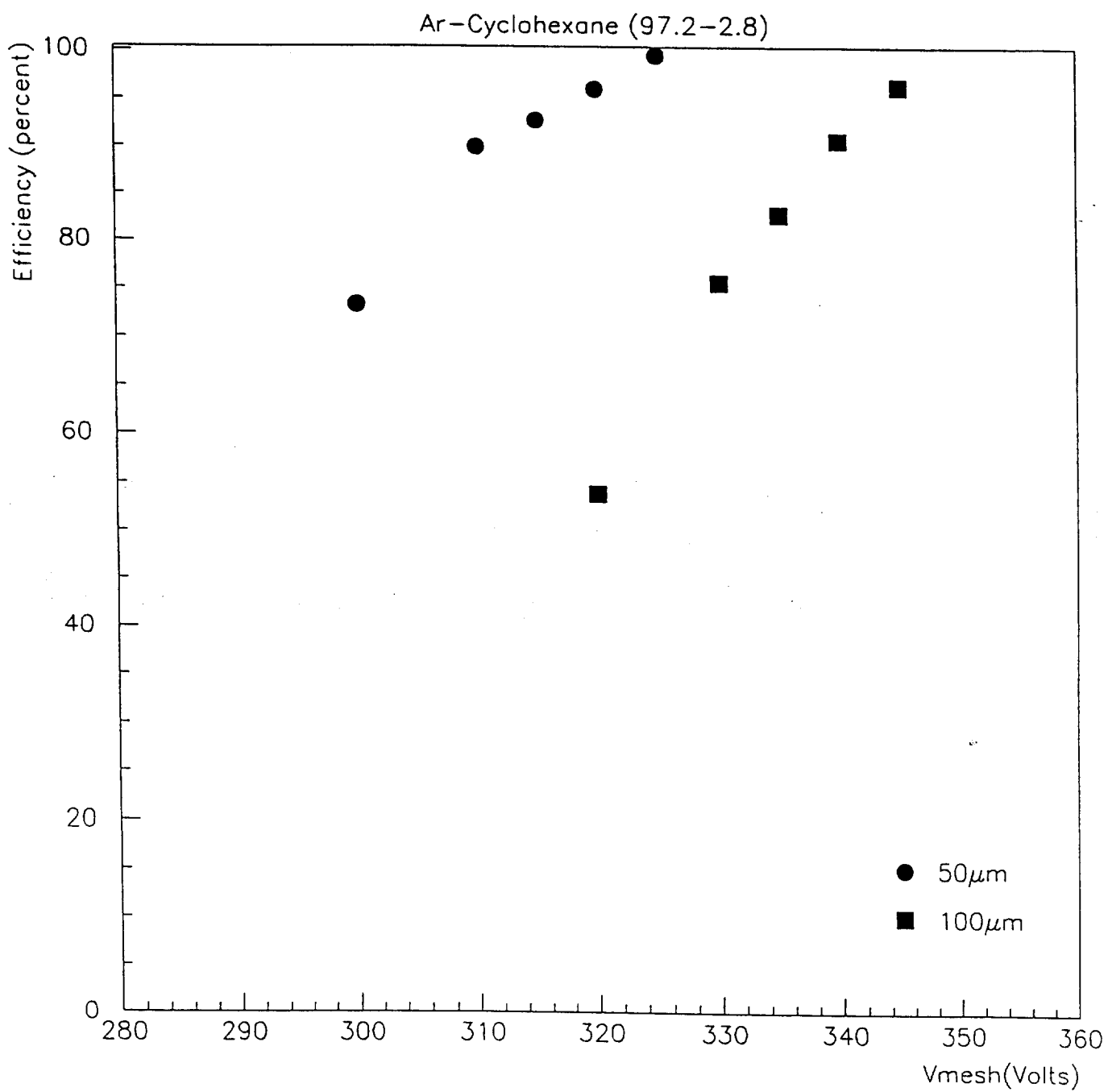


Fig. 22

